Delft University of Technology
Dept. of Aerospace Engineering
Delft
The Netherlands

Technological Laboratory TNO
Rijswijk
The Netherlands

Report LR-252
Report no. TL R 3050-II

RESULTS OF L^*-INSTABILITY EXPERIMENTS WITH DOUBLE BASE ROCKET PROPELLANTS II

by

R. S. de Boer
H. F. R. Schöyer
H. Wolff

DELFT/RIJSWIJK - THE NETHERLANDS
September 1977

Delft University of Technology
Dept. of Aerospace Engineering
Delft
The Netherlands

Technological Laboratory TNO
Rijswijk
The Netherlands

Report LR-252
Report no. TL R 3050-II

RESULTS OF L^*-INSTABILITY EXPERIMENTS WITH DOUBLE BASE ROCKET PROPELLANTS II

by

R. S. de Boer
H. F. R. Schöyer
H. Wolff

DELFT/RIJSWIJK - THE NETHERLANDS
September 1977

DELFT UNIVERSITY OF TECHNOLOGY
DEPT. OF AEROSPACE ENGINEERING
Kluyverweg 1
DELFT
THE NETHERLANDS

TECHNOLOGICAL LABORATORY TNO
Lange Kleiweg 137
P.O. Box 45
RIJSWIJK
THE NETHERLANDS

Requested by : Director of Technol. Lab. TNO; letter no. 5337, dated 29-10-1971, and H. Wittenberg of Delft University of Technology; letter no. HW/cvd/VTH, 18/4.4.2./72, dated 5-1-1972.

Subject : Results of L^*-Instability Experiments With Double Base Rocket Propellants II.

Sample description : JPN propellant disks, manufactured from grains (Mk 18 Mod 0; lots SUN 2658, 2676, 2679, and 2729; year of manuf.: 1952) of 5-in. HVARs (TL 27/72, 252/72, 239/73, and 252/73).
ARP propellant disks, manufactured from grain no. 65 (lot RAD-2-18) of an Honest-John-rocket (TL 536/64).

Continuous Working Program
Technol. Lab., 1977/1981, ref. no.: 1.2.2
TL assignment no. : R 3050 (9095)
LRT report no. : LR-252
TL report no. : R 3050-II
Date : September 1977
Authors : R.S. de Boer, H.F.R. Schöyer, and H. Wolff.

Investigation performed under supervision of : R.S. de Boer, H.F.R. Schöyer, and H. Wolff.
by : T. Dijkman and B.A.C. Ambrosius.

Summary

A series of oscillatory combustion experiments has been conducted to detect the sensitivity of double base rocket propellants for low frequency oscillations. The experiments are a continuation of earlier work by De Boer and Schöyer, and the ignition technique developed earlier, again proved to be reliable and gave reproducible results.
In the experiments reported herein two regions in the L^* - plane were found where ARP propellant was apt to oscillate:
0,15 MPa < $\bar{p}$ < 0,4 MPa with 0,25 m < L^* < 0,8 m and 1,4 MPa < $\bar{p}$ < 4 MPa with 0,25 m < L^* < 1,6 m (L^* = characteristic length of the combustion chamber; $\bar{p}$ = mean pressure at oscillation). No oscillations have been observed with JPN propellant. It is conceivable that this is due to the absence of an ignition peak.
Tests that yielded oscillations are reported in detail in this report both in tabular and in graphical form.
From the data the effective growth constants have been deduced and postulating various models for damping in the combustion chamber, it has been possible to estimate the growth constant of ARP propellant. The best correlation has been obtained by assuming volumetric damping. Correlation of the response function with $\bar{p}$ has been found to be weak, like the correlations between mean pressure at oscillation and L^* and between frequency and L^*. Both 5 and 10 cm L^* burners have been used; it is of interest to note that the data scatter for the 5 cm and 10 cm burner is of the same order as the data scatter between the 5 cm and 10 cm burners. Therefore the results of the different burners agree rather well. Very good correlation has been found between frequency and mean pressure and over a much wider pressure range than previously reported. Moreover, a high frequency - low pressure correlation has been observed which, to the authors' knowledge, has never been reported earlier.

Table of contents

1. Nomenclature

A	area
C	constant
D	diameter
d	diameter
F	frequency
G	ignition mixture weight
L^*	characteristic length
ℓ	distance from propellant surface to nozzle end plate
n	number of times
P	period
p	pressure
R	gas constant
R_b	response function
r	linear burning rate
T	temperature
T	period
T	term in Eqs. (6-6) and (6-7)
t	time
V	volume
α	growth constant
Γ	function of γ (Vandenkerckhove function)
γ	ratio of specific heats
Δ	increment; perturbed value
δ	number $1 \leq \delta \leq \gamma$
ω	angular frequency

Subscripts and superscripts

b	propellant surface; burning
c	chamber
d	damping; decay
eff	effective

f	final
i	initial; ignition
im	minimum value during period i
max	maximum
0	at time t=0
$(\bar{\ })$	mean value
$(\ )^{(i)}$	imaginary part
$(\ )^{(r)}$	real part

2. Introduction

For several years, the Department of Aerospace Engineering of Delft University of Technology and the Technological Laboratory TNO at Rijswijk conduct investigations of low frequency combustion instability, also called L^* instability. De Boer and Schöyer[1] have reported experiments with double base propellants where they found that JPN propellant may oscillate in a limited $\bar{p} - L^*$ region, but no ARP oscillations had been observed.

When Wolff was introduced to the experiments during a sabbatical period spent at Delft University, L^* oscillations of ARP propellant were observed. The experiments were conducted in an L^*-pressure region not previously investigated and prompted the investigators to continue their search for L^* oscillations of double base propellants. No oscillations were noted with JPN in the newly investigated regions; however, ARP propellant yielded oscillations during seven experiments. The results of these experiments proved highly interesting because a new pressure--frequency correlation was identified, and a pressure-frequency correlation of a type previously reported was observed over a much larger pressure range than noted in the open literature.

The growth constant of ARP propellant may be estimated on the assumption of linear damping and it was determined that the maximum is a few tens per second.

This report presents detailed information on the experiments. The reader who wants further specific information about the L^* burners, the ignition methods, the propellant, and oscillatory behavior of JPN propellant, is referred to De Boer and Schöyer[1].

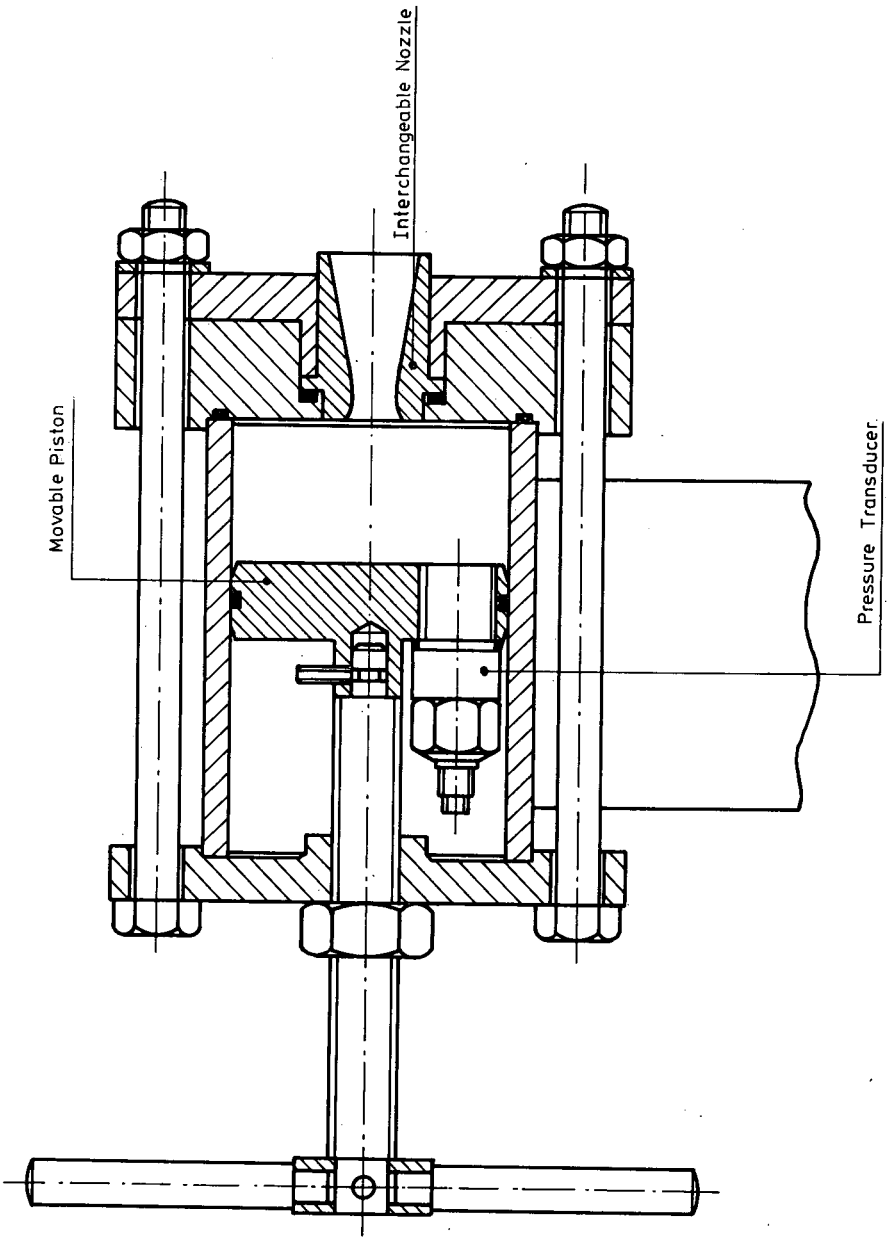

Figure 1. Schematic of the 5 cm L* burner.

3. Experimental system

The experimental system which was used with these tests was basi-
-cally the same as reported in Reference 1, except for a tape recorder and some new nozzles.

3.1. Test apparatus

In Reference 1 some theoretical consideratious about L^* oscillations were presented, together with an extensive description of the L^* burners. For a full description of the L^* burners the reader is referred to Section 5 of Reference 1. In the present tests two L^* burners were used, one with a 5 cm chamber diameter and one with a 10 cm chamber diamter, called the 5 cm and 10 cm L^* burner, respectively.
Figure 1 is a schematic of the 5 cm L^* burner. The 10 cm burner is similar. Table 1 describes the different nozzles necessary to obtain a wide range of steady state chamber pressures.

3.2. Instrumentation

Only a tape recorder was added to the instrumentation as described in Reference 1.

Tape recorder:

HEWLETT-PACKARD four channel instrumentation tape recorder, model 3960. Tape speeds: 15 inch/s, 15/4 inch/s and 15/16 inch/s. This unit permits aquisition of all pressure data plus transducer calibration on magnetic tape, and offers the following advantages:

- Magnetic tape is better suited for long term data storage than the photographic paper used in an ultraviolet oscillograph.
- Magnetic tape permits play back. When replaying the tape it is possible, by using different speeds and different amplifier settings or galvanometers to "stretch" or "compress" the scales. This results in more accurate measurements when data reduction is done "by hand", and one can produce an oscillograph of convenient size to see at a glance the pressure history.

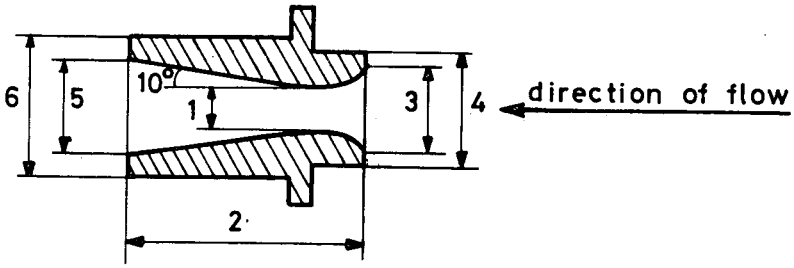

Figure 2. Schematic of a typical nozzle. Numbers refer to dimensions presented in Table 1

Table 1

Survey of nozzles available for 5 cm and 10 cm L* burners (see Fig. 2)

	Dimension no.					
nozzle no.	1 (mm)	2 (mm)	3 (mm)	4 (mm)	5 (mm)	6 (mm)
2	2,0	30,0	9,2	18,01*	11,0	20,01*
3	2,95	30,0	12,0	18,00*	12,0	20,04*
4A	3,9	30,1	12,45	18,01*	12,6	20,01*
4B	4,2	30,05	10,0	18,00*	12,5	19,99*
4C	4,45	30,0	8,0	18,01*	12,8	20,00*
4D	4,7	30,05	8,0	18,02*	13,1	20,01*
5A	5,05*	30,0	8,2	18,01*	13,0	20,02*
5B	5,21*	30,0	13,5	18,00*	13,2	20,00*
6	6,01*	29,85	12,5	18,01*	15,0	20,01*
7A	7,02*	29,95	14,95	18,01*	16,0	20,01*
7B	7,03*	30,0	13,2	18,00*	14,9	20,00*
8	7,84*	30,0	15,0	18,01*	16,5	20,01*
9A	9,03*	29,9	14,4	18,01*	17,8	20,01*
9B	9,26*	30,05	13,3	17,99*	17,3	19,98*
9C	9,50*	30,05	13,4	17,99*	17,1	19,99*
9D	9,80*	30,0	13,3	17,98*	17,3	19,98*
10A	10,13*	30,0	15,5	18,01*	18,6	20,01*
10B	10,54*	29,95	15,6	18,00*	18,0	20,00*

- The signal recorded on magnetic tape can be digitalized; a necessity for computerized data reduction. A computer program for this type of data reduction is being developed at the Department of Aerospace Engineering of D.U.T.

4. Experimental results and discussion

Twentyfour experiments with double base propellants were conducted to determine whether oscillatory combustion occurred and if so under what conditions. Five were with JPN propellant and 19 with ARP propellant. Ignition was accomplished by means of an electrical resistance wire, embedded in a pyrotechnic lacquer and is referred to as type L in Reference 1, Section 7. These experiments were a continuation of the investigations reported in Reference 1.

Tests with JPN propellant disks in the 5 cm L^* burner

In previous tests (Ref. 1, tests nos. 249, 253, 254, and 303B), oscillatory combustion was observed with JPN propellant disks in the 5 cm L^* burner.

Table 2 summarizes the most important independent test variables: L^*, d_t, and $\bar{p}$. An unsuccessful attempt was made to repeat the L^* - $\bar{p}$ conditions as closely as possible, using a slightly different nozzle, d_t = 5,05 mm. These tests nos. 931 and 932 produced chuffing, but no oscillations although the mean pressures were in the same range as the tests of Table 2.

Table 2

Summary of independent test variables for oscillatory combustion: Reference 1, test nos. 249, 253, 254, 303B (D = 5 cm; Propellant: JPN)

Test no.	L^* range (m)	d_t (mm)	$\bar{p}$ (MPa)	remarks
249	4,19 - 5,15	5,18	1,4	high ignition peak
253	3,73 - 4,66	5,18	0,9	" " "
254	4,19 - 5,11	5,18	1,0	" " "
303B	5,12 - 5,20	5,18	0,9	extinguishment

Table 3

Results of L^* burner tests (D = 5 cm; propellant: JPN) *)

Test no.	T [°C]	propellant disk no. (thickness) [mm]	ℓ (d_t) [mm]	L_i^* (L_f^*) [m]	G ignition mixture weight [g]	p_i [MPa]	p_{max} ($\bar{p}$) [MPa]	t_b [s]	chuffing	remarks
931	17	8 (20,1)	45 (5,05)	4,41 (6,19)	1,75	∿0,2	1,13 (1,1)	3,8	yes	burnt surface oblique; residual propellant 2 mm.
932	17	9 (20,0)	45 (5,05)	4,41 (6,08)	1,78	0,13	1,39 (1,1)	3,6	yes	burnt surface oblique; residual propellant 3 mm.

*) In all experiments, discussed in this report silicone rubber (SR) was used as inhibitor. Ignition always took place by means of an electrical resistance wire embedded in a pyrotechnic lacquer, designated as type L in Reference 1.

(a)

Test no.: 931,
932,
933.

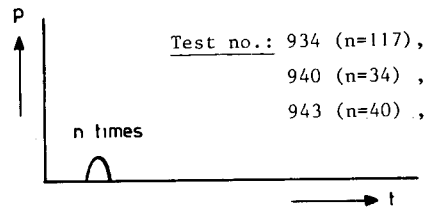

(b)

Test no.: 934 (n=117), 938 (n=93), 939 (n=42),
940 (n=34) , 941 (n=88), 942 (n=48),
943 (n=40) , 947 (n=72), 954 (n=105).

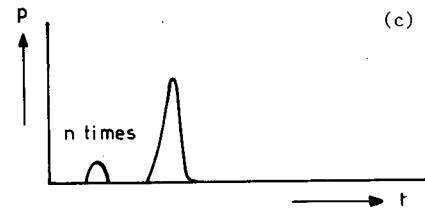

(c)

Test no.: 935 (n=86),
945 (n=90),
948 (n=104).

Figure 3. Schematic representation of pressure histories recorded during tests. From Tables 3, 4, 5 and 6 (not to scale).

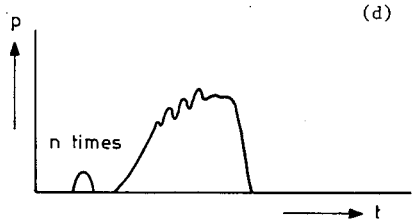

(d)

Test no.: 936 (n=58),
952 (n=81),
956 (n=36).

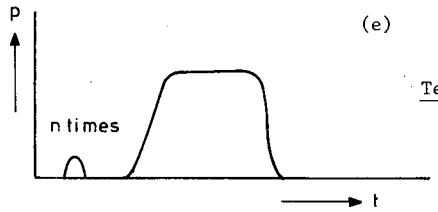

(e)

Test no.: 949 (n=2).

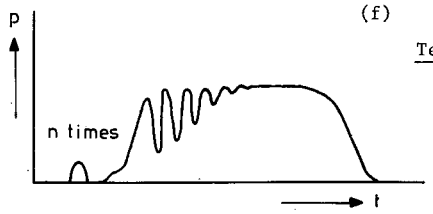

(f)

Test no.: 950 (n=4),
951 (n=6),
953 (n=6),
955 (n=4).

The data listed in Table 3 showed that the L^* was somewhat larger than during the previous tests of Table 2. Moreover, in tests nos. 249, 253, and 254 there was an ignition peak that may have triggered oscillations and this ignition peak did not occur in tests nos. 931 and 932. This may indicate that the occurrence of the bulk mode oscillations was very sensitive to the magnitude of L^* and the presence of ignition peaks. Sketches of the pressure histories, Fig. $3^{(a)}$, showed that in both cases the propellant chuffed only once, followed by a more or less regular combustion.

Test with JPN propellant disks in the 10 cm L^* burner

Tests nos. 933, 942, and 943 were conducted to determine whether oscillatory combustion occurred in the 10 cm L^* burner in the 1,5 MPa region and if so under what conditions. The data summarized in Table 4 indicate that only during test no. 933 the conditions were similar to those of the tests of Table 2. The pressure history of test no. 933, schematically shown in Fig. $3^{(a)}$, showed that the propellant chuffed only once, followed by a stable, non-oscillatory combustion whereas in tests nos. 942 and 943 with extremely small L^* only chuffing occurred as noted in Fig. $3^{(b)}$.

Tests with ARP propellant disks in the 5 cm L^* burner

Table 5 summarizes experiments with ARP propellant in the 5 cm L^*-burner. During previous experiments [1] no oscillatory behavior was observed, but test no. 936, at a pressure level not previously investigated, yielded pressure oscillations and prompted the investigators to continue the search for L^* oscillations of ARP propellant. Chuffing, followed by pressure oscillations was then found in tests nos. 955 and 956.
To ascertain whether pressure spikes triggered L^* oscillations, two propellant disks were bonded to each other with a layer of ignition mixture, type L (Reference 1, Section 7). The concept was that the flame front reaching the igniter paste between the two disks, would produce a pressure peak, which in turn might trigger L^* oscillations. This was done in tests nos. 945, 946, and 947; however, as apparent in Table 5,

Table 4

Results of L^* burner tests (D = 10 cm; propellant: JPN)

Test no.	T [°C]	propellant disk no. (thickness) [mm]	ℓ (d_t) [mm]	L_i^* (L_f^*) [m]	G ignition mixture weight [g]	p_i [MPa]	p_{max} ($\bar{p}$) [MPa]	t_b [s]	chuffing	remarks
933	17	174 (19,5)	45 (10,13)	4,39 (6,29)	3,08	0,20	1,67 (1,5)	3,3	yes	
942	20	200 (17,3)	2,5 (9,80)	0,26 (2,06)	2,85	0,20	0,87 (0,45)	32,2	yes	
943	20	201 (18,2)	2,5 (10,13)	0,24 (2,02)	2,57	0,25	0,99 (0,50)	31,6	yes	

Table 5

Results of L^* burner tests (D = 5 cm; propellant: ARP)

Test no.	T [°C]	propellant disk no. (thickness) [mm]	ℓ (d_t) [mm]	L_i^* (L_f^*) [m]	G ignition mixture weight [g]	p_i [MPa]	p_{max} ($\bar{p}$) [MPa]	t_b [s]	chuffing	remarks
935	17	73 (20,1)	2,5 (4,70)	0,28 (2,56)	1,76	0,37	∿2,0 (0,40)	15,2	yes	
936	17	74 (19,55)	2,5 (4,70)	0,28 (2,50)	1,89	0,37	2,48 ∿(2,50)	11,2	yes	oscillatory combustion in three successive periods.
938	20	72 (14,1)	2,5 (4,70)	0,28 (1,88)	1,70	0,38	0,54 (0,30)	23,3	yes	
939	20	102 (14,1)	8,5 (4,70)	0,96 (2,56)	1,93	0,18	0,57 (0,30)	18,4	yes	
940	20	112 (10,1)	13,5 (4,70)	1,53 (2,67)	1,72	0,22	0,63 (0,35)	11,2	yes	
941	20	108 (10,1)	2,5 (4,70)	0,28 (1,43)	1,70	0,37	0,66 (0,35)	13,7	yes	
945	20	103+111 (19,9+10,1)	2,5 (4,70)	0,28 (3,68)	1,35	0,13	3,62 (1,6)	22,5	yes	ignition mixture, type L, G=2,97 g between two propellant disks.
946	20	77+107 (19,85+9,8)	9,0 (4,70)	1,02 (2,13)	1,49	-	-	-	yes	ignition mixture, type L, G=3,26 g between propellant disks. Residual propellant 19,9 mm. No pressure measurement.

Table 5

Results of L^* burner tests (D = 5 cm; propellant: ARP) (cont'd)

Test no.	T [°C]	propellant disk no. (thickness) [mm]	ℓ (d_t) [mm]	L_i^* (L_f^*) [m]	G ignition mixture weight [g]	p_i [MPa]	Pmax ($\bar{p}$) [MPa]	t_b [s]	chuffing	remarks
947	20	76+106 (20,05+10,15)	2,5 (4,70)	0,28 (1,43)	1,39	0,24	0,44 (0,25)	13,3	yes	ignition mixture, type L, G=4,11 g between propellant disks. Residual propellant 20,1 mm.
948	20	118 (26,6)	2,5 (4,70)	0,28 (3,29)	1,54	0,28	4,88 (2,1)	21,2	yes	
954	22	75 (20,1)	2,7 (4,70)	0,31 (2,58)	1,54	0,40	0,53 (0,40)	26,0	yes	
955	22	76 (20,0)	2,2 (4,20)	0,31 (3,15)	1,28	0,27	3,95 (3,6)	2,5	yes	oscillatory combustion
956	22	77 (19,0)	2,5 (4,45)	0,32 (2,71)	1,33	0,27	3,19 (3,0)	5,8	yes	oscillatory combustion

Table 5 (cont'd)

no oscillations were observed. In two cases, tests nos 946 and 947, the second disk did not burn but it was not clear whether or not this was a case of dp/dt extinguishment. From Table 5 it is evident that the occurrence of L^* oscillations depended on factors other than just the mean presuure level, i.e. the nozzle throat diameter, d_t, and the set L_i^*. Comparing data from tests nos. 935 and 936, it was clear that, while the independent variables L_i^* and d_t were the same in both cases, the outcome differed considerably as shown in Fig. $3^{(a),(c)}$. On the other hand, it is well known that chuffing often preceeds L^* oscillations. Figs. 4 through 6 show the pressure oscillations observed during tests nos. 936, 955, and 956. In test no. 936 pressure oscillations occurred during three successive periods, but only the last and strongest group of oscillations, denoted 936^{III} is depicted in Fig. 4. It was noted that with all three tests the pressure oscillations were preceeded by a pressure plateau, at a pressure level much lower than that dictated by equilibrium considerations. The period, amplitude, and effective growth constant of the oscillations were determined as shown in Section 5, Data reduction.

Tests with ARP propellant disks in the 10 cm L^* burner

Table 6 summarizes the results of experiments with ARP propellant in the 10 cm L^* burner. Of the six experiments, four yielded oscillations of the type illustrated in Fig. $3^{(d),(f)}$, and in all cases chuffing was observed. Again it was noted that oscillations occurred only in a very limited range of L^* and pressure levels: for example, the L^* during test no. 934 ranged from 0,28 m to 2,22 m, while for tests nos. 950, 951, and 953 the L^* ranged from 0,31 m to 3,37 m. The only difference was that test no. 934 used a nozzle with d_t = 9,50 mm while the other three experiments were conducted with a slightly smaller nozzle, d_t = 9,03 mm. Tests nos. 950, 951, and 953 clearly yielded oscillations, as shown in Figs. 7, 8, and 9, and demonstrated the reproducibility of the L^* oscillations. Test no. 952, Fig. 10, with approximately the same L^* range as the other tests was conducted with nozzle d_t = 9,26 mm, which was just in between the nozzles used with tests nos. 934, 950, 951, and 953. The results were also more or less "in between" as the oscillations were less

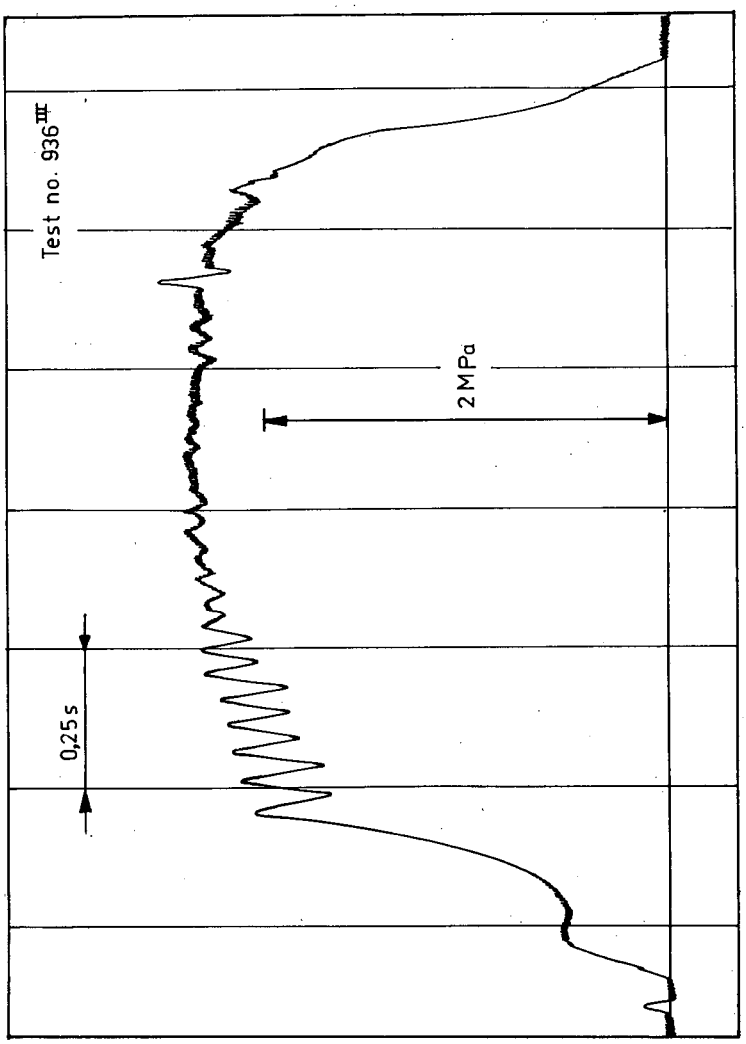

Figure 4. Pressure history for test no. 936 (third group of oscillations)(D = 5 cm).

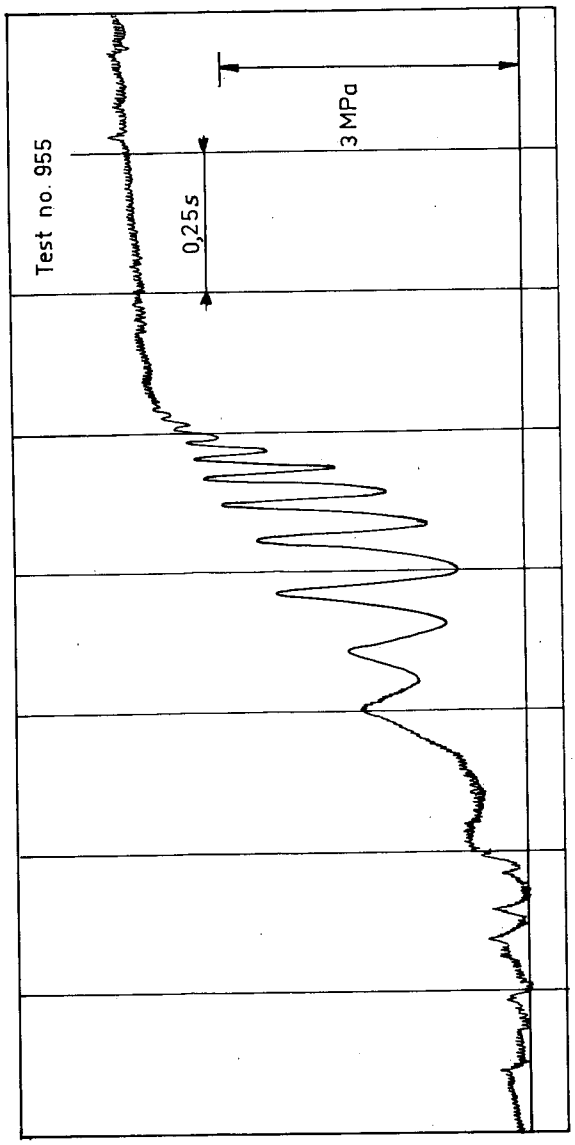

Figure 5. Part of the pressure history for test no. 955 (D = 5 cm).

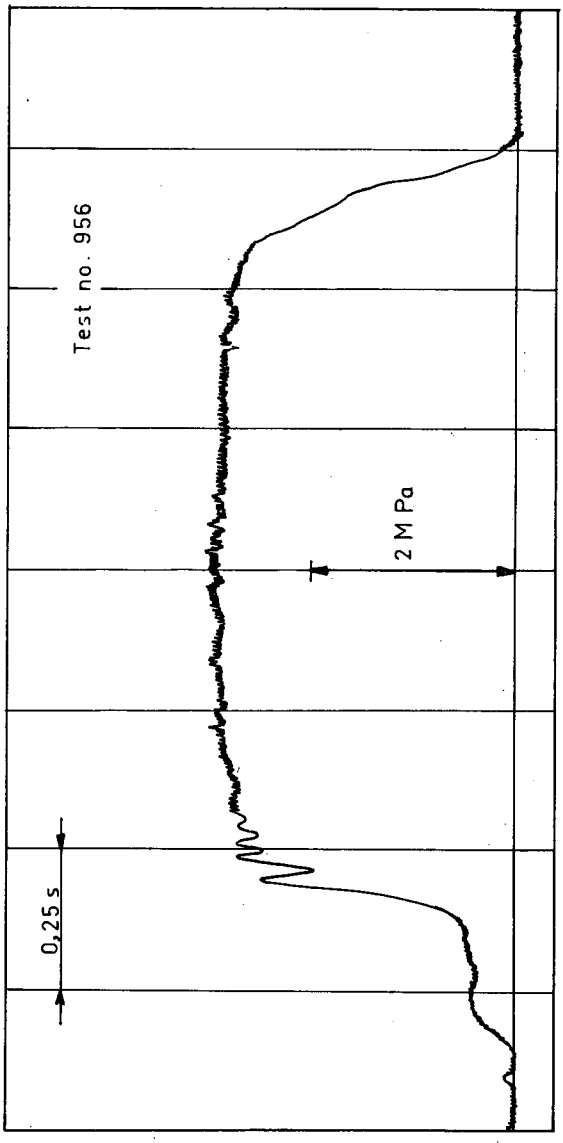

Figure 6. Pressure history for test no. 956 (D = 5 cm).

Table 6

Results of L^* burner tests (D = 10 cm; propellant: ARP)

Test no.	T [°C]	propellant disk no. (thickness) [mm]	ℓ (d_t) [mm]	L_i^* (L_f^*) [m]	G ignition mixture weight [g]	p_i [MPa]	p_{max} ($\bar{p}$) [MPa]	t_b [s]	chuffing	remarks
934	17	171 (17,5)	2,5 (9,50)	0,28 (2,22)	4,74	0,13	0,60 (0,35)	27,9	yes	
949	20	205 (19,3)	2,5 (7,02	0,51 (4,42)	4,08	0,30	8,75 (8,1)	1,6	yes	
950	20	206 (21,2)	2,5 (9,03)	0,31 (2,91)	3,74	0,20	3,25 (3,0)	2,6	yes	oscillatory combustion
951	22	208 (22,2)	2,5 (9,03)	0,31 (3,03)	3,76	0,35	3,76 (3,3)	2,3	yes	oscillatory combustion
952	22	207 (16,0)	2,5 (9,26)	0,29 (2,16)	3,75	0,20	≈3,00 ≈(2,9)	16,1	yes	oscillatory combustion
953	22	209 (25,0)	2,5 (9,03)	0,31 (3.37)	4,04	0,20	3,99 (3,5)	2,6	yes	oscillatory combustion

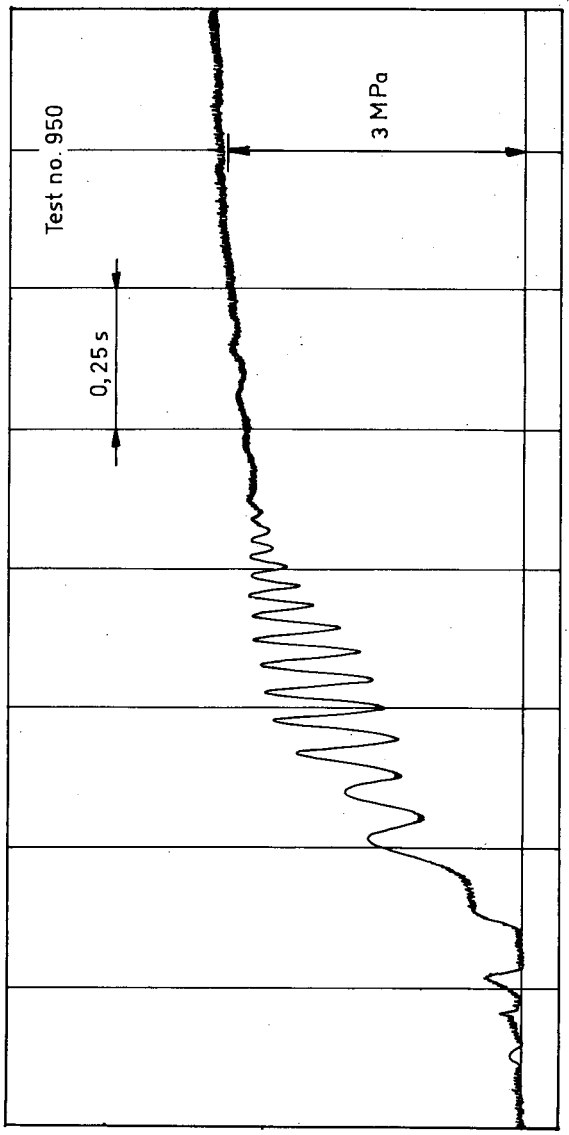

Figure 7. Part of the pressure history for test no. 950 (D = 10 cm).

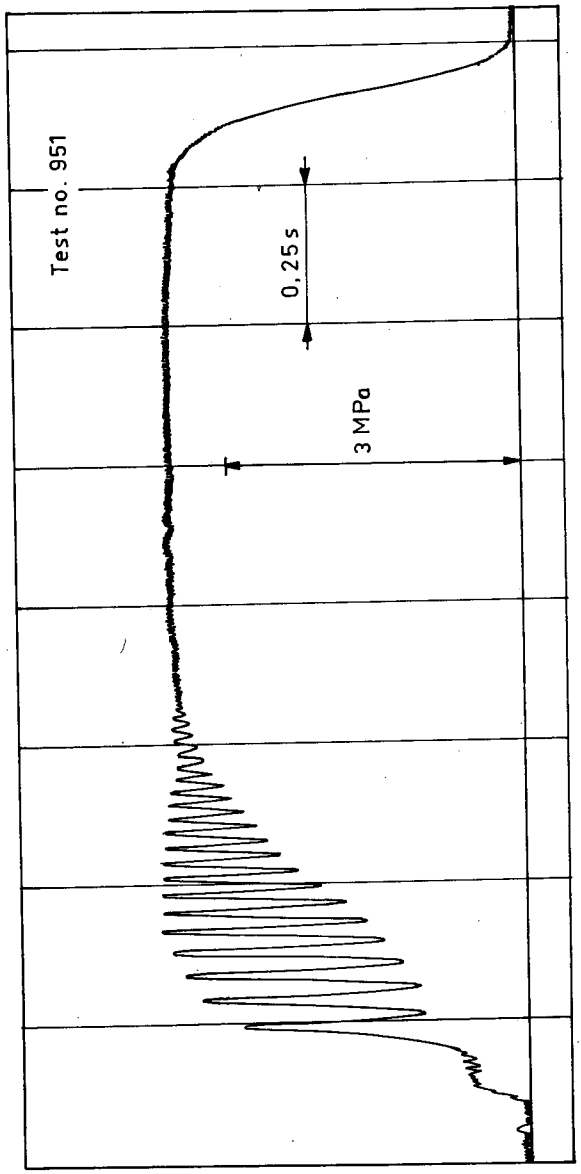

Figure 8. Pressure history for test no. 951 (D = 10 cm).

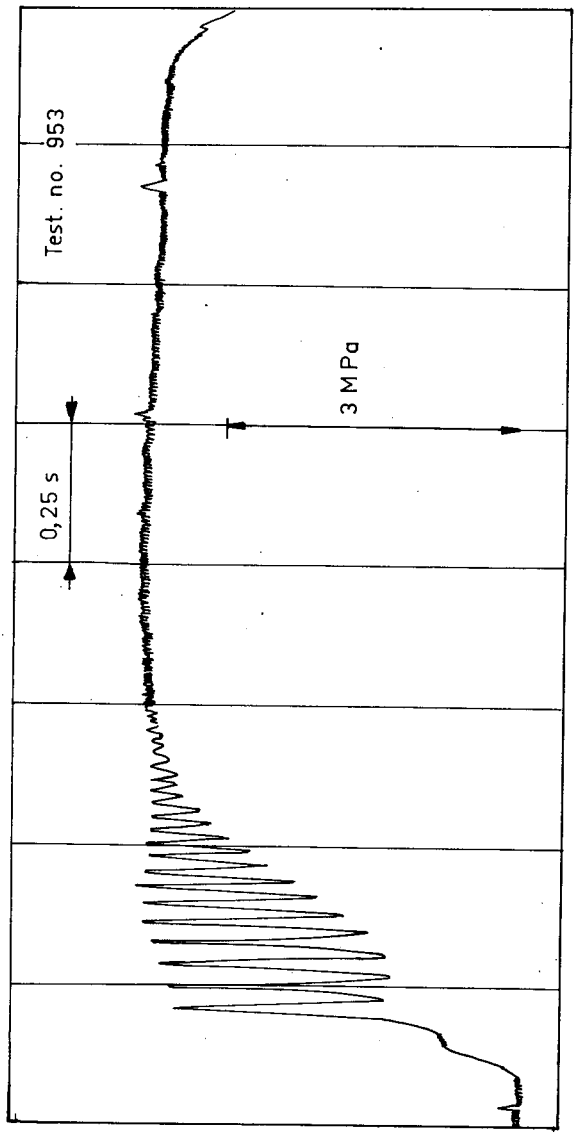

Figure 9. Part of the pressure history for test no. 953 (D = 10 cm).

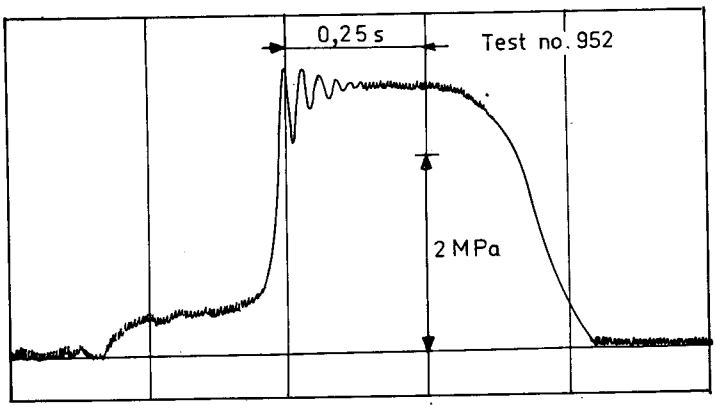

Figure 10. Pressure history for test no. 952 (D = 10 cm).

pronounced and only of a short duration. Test no. 949 which used a still smaller nozzle, resulted in a higher equilibrium pressure, and after chuffing twice, progressed to steady burning at a pressure level of ∿ 8 MPa, as shown in Fig. $3^{(a)}$. Comparing the results of the oscillatory combustion experiments in the 10 cm L^* burner with those in the 5 cm L^* burner, it was noted that again the oscillations were preceeded by a pressure plateau at a level much lower than the equilibrium pressure level. All oscillatory combustion occurred at pressures, approximately 2,5 MPa to 3,5 MPa, and at L^* aproximately 0,3 m to 3 m. A more detailed analysis of the results of those experiments that showed oscillatory combustion is presented in Section 5, Data reduction.

5. Data reduction

The measured pressure was recorded on photographic paper by an oscillograph. The "zero" pressure level corresponded to ambient pressure (∿0,1 MPa). Recorded pressure and time were measured with an ordinary scale; therefore the accuracy was ∿0,25 mm. To analyze test results, an arbitrary "zero" time level was chosen as the reference level for evaluation of a particular part of the pressure record. Time and pressure values, measured in mm, as listed in Tables 7 through 11 were for tests nos. 936, 950 through 953, 955, and 956. The measured pressures were the peak pressure and the minimum pressure and were used to determine the mean pressure and the pressure amplitude in mm.

From these pressure values in mm, the actual pressure in MPa was calculated. Time listed in the second and third columns was not an absolute time. Frequency F, the reciprocal of time period P, was calculated from the time differences. Where groups of oscillations occurred in a single test, typically test no. 936, different reference times were selected for each group of oscillations analyzed. The procedure is evident in Table 7 for groups of oscillations, 936^{I}, 936^{II}, and 936^{III}. Figure 11 illustrates the definitions used for data reduction. The time to which a variable is related is the time of the youngest pressure peak. Thus, the time interval between peaks at T_i and T_{i+1} is by definition,

Table 7. Results of L^* burner test no. 936 (D = 5 cm; propellant: ARP)

Test no. (1)	Time		Period		Peak Pressure		Minimum Pressure		Pressure Amplitude		Mean Pressure		Estimated L^*	F	$\Delta p/\bar{p}$
	(mm)	(s)	(mm)	(s)	(mm)	(MPa)	(mm)	(MPa)	(mm)	(MPa)	(mm)	(MPa)	(m)	(s^{-1})	
936^{I}	22	0,0423	9,2	0,0177	4,5	0,1328	4,5	0,1328	0	0	4,5	0,1328	0,800	56,50	0
	31,2	0,0600	8,8	0,0169	9	0,2656	9	0,2656	0	0	9	0,2656	0,804	59,17	0
	40	0,0769	7	0,0135	12,5	0,3689	12,3	0,3630	0,1	0,0030	12,4	0,3660	0,810	74,07	$8,2 \times 10^{-3}$
	47	0,0904	9,2	0,0177	14	0,4192	12,5	0,3689	0,75	0,0221	13,25	0,3910	0,816	56,50	$5,65 \times 10^{-2}$
	56,2	0,1081	8,3	0,0160	13	0,3837	12,2	0,3600	0,4	0,0118	12,6	0,3719	0,824	62,50	$3,17 \times 10^{-2}$
	64,5	0,1240	10,3	0,0198	13,1	0,3866	10	0,2951	1,55	0,0457	11,55	0,3409	0,831	50,51	$1,34 \times 10^{-2}$
	74,8	0,1438			12								0,839		
936^{II}	12	0,0231	9,2	0,0177	4,8	0,1417	4,2	0,1240	0,3	0,0089	4,5	0,1328	0,846	56,50	$6,7 \times 10^{-2}$
	21,2	0,0408	11,8	0,0227	8,8	0,2597	7	0,2066	0,9	0,0266	7,9	0,2331	0,852	44,05	$1,14 \times 10^{-1}$
	33	0,0635			12								0,859		
936^{III}	17,5	0,0337	28	0,0538	72	2,1249	60	1,7707	6	0,1771	66	1,9478	1,060	18,59	$9,09 \times 10^{-2}$
	45,5	0,0875	26	0,0500	74,5	2,1987	61	1,8002	6,75	0,1992	68,75	2,0290	1,118	20	$9,82 \times 10^{-2}$
	71,5	0,1375	24,5	0,0471	76,5	2,2577	65,5	1,9330	5,5	0,1623	71	2,0954	1,173	21,23	$7,75 \times 10^{-2}$
	96	0,1846	23	0,0442	76,5	2,2577	67	1,9773	4,75	0,1402	71,75	2,1175	1,226	22,51	$6,62 \times 10^{-2}$
	119	0,2288	24	0,0462	78	2,3019	67,5	1,9921	5,25	0,1549	72,75	2,1470	1,276	21,65	$7,21 \times 10^{-2}$
	143	0,2750	20,5	0,0394	81	2,3905	72,5	2,1396	4,25	0,1254	76,75	2,2651	1,329	25,38	$5,54 \times 10^{-2}$
	163,5	0,3144	24,5	0,0471	81	2,3905	73,5	2,1691	3,75	0,1107	77,25	2,2798	1,375	21,23	$4,86 \times 10^{-2}$
	188	0,3615	18,5	0,0356	81	2,3905	79	2,3315	1	0,0295	80	2,3610	1,430	28,09	$1,25 \times 10^{-2}$
	206,5	0,3971			81	2,3905	78	2,3019	1,5	0,0449	79,5	2,3462	1,473		$1,91 \times 10^{-2}$

(1) 936^{I} : first group of oscillations in test 936
936^{II} : second group of oscillations in test 936
936^{III}: third group of oscillations in test 936

Table 8. Results of L^* burner test no. 950 (D = 10 cm; propellant: ARP)

Test no.	Time		Period		Peak Pressure		Minimum Pressure		Pressure Amplitude		Mean Pressure		Estimated $L^{*(1)}$ (m)	F (s^{-1})	$\Delta p/\bar{p}$
	(mm)	(s)	(mm)	(s)	(mm)	(MPa)	(mm)	(MPa)	(mm)	(MPa)	(mm)	(MPa)			
950	79,5	0,194	34	0,083	30	1,747	20	1,165	5	0,291	25	1,456	0,017	12,05	0,200
	113,5	0,277	27,5	0,067	33,5	1,951	24	1,398	4,75	0,277	28,75	1,674	0,099	14,90	0,165
	141	0,344	24	0,059	42,5	2,475	23,5	1,369	9,5	0,553	33	1,922	0,171	17,07	0,288
	165	0,403	21,5	0,052	47	2,737	27	1,572	10	0,582	37	2,155	0,240	19,05	0,270
	186,5	0,454	19,7	0,048	49	2,854	29	1,689	10	0,582	39	2,271	0,304	20,79	0,256
	206,2	0,509	18,8	0,046	50	2,912	31	1,805	9,5	0,553	40,5	2,359	0,365	21,79	0,235
	225	0,549	17	0,042	50	2,912	34	1,980	8	0,466	42	2,446	0,424	24,09	0,190
	242	0,591	15	0,037	50	2,912	40	2,330	5	0,291	45	2,621	0,480	27,31	0,111
	257	0,627	14,5	0,035	51	2,970	42	2,446	4,5	0,262	46,5	2,708	0,531	28,25	0,097
	271,5	0,663	14,5	0,035	50	2,912	44,2	2,574	2,9	0,169	47,1	2,743	0,580	28,25	0,062
	286	0,698	12,5	0,031	50	2,912	47	2,737	1,5	0,087	48,5	2,825	0,629	32,77	0,031
	298,5	0,729	13	0,032	51	2,970	47	2,737	2	0,116	49	2,854	0,673	31,51	0,041
	311,5	0,760			50	2,912							0,719		

(1) Calculated from t_f, backwards. If L^* was calculated from t_i then at the first pressure peak, L^* = 0,427 m as by adding 0,410 m to the results in the column Estimated L^*, one obtaines the L^* values as based on L_i^*. The L^* = 0,410 m is based on the measured distance from the initial propellant surface to the nozzle end plate.

Table 9. Results of L^* burner test no. 951 (D = 10 cm; propellant: ARP)

Test no.	Time		Period		Peak Pressure		Minimum Pressure		Pressure Amplitude		Mean Pressure		Estimated $L^{*(1)}$	F	$\Delta p/\bar{p}$
	(mm)	(s)	(mm)	(s)	(mm)	(MPa)	(mm)	(MPa)	(mm)	(MPa)	(mm)	(MPa)	(m)	(s^{-1})	
951	6,8	0,0135	5,8	0,0115	7	0,404	7	0,404	0	0	7	0,404	0,285	87,1	0
	12,6	0,025	5,4	0,0107	9	0,519	8	0,462	0,5	0,028	8,50	0,490	0,291	93,5	0,059
	18	0,0356			11,5	0,663							0,297		
	36,5	0,0723	6,5	0,0129	12	0,692	11	0,635	0,5	0,028	11,50	0,663	0,321	77,7	0,049
	43	0,0851	6	0,0119	12,5	0,721	12,5	0,721	0	0	12,50	0,721	0,329	84,2	0
	49	0,0970			16	0,923							0,337		
	78,5	0,1554	23,5	0,0465	54	3,115	21,5	1,240	16,25	0,937	37,75	2,178	0,393	21,5	0,430
	102	0,2020	23	0,0455	61	3,519	22,5	1,298	19,25	1,111	41,75	2,409	0,451	22	0,461
	125	0,2475	21	0,0416	65	3,750	25,5	1,471	19,75	1,139	45,25	2,610	0,510	24	0,436
	146	0,2891	19	0,0376	67	3,865	28	1,615	19,50	1,125	47,50	2,740	0,567	26,6	0,411
	165	0,3267	18,5	0,0366	68,5	3,952	32	1,846	18,25	0,053	50,25	2,899	0,620	27,3	0,363
	183,5	0,3634	15,5	0,0307	69,5	4,009	36	2,077	16,75	0,966	52,75	3,043	0,673	32,6	0,318
	199	0,3941	15	0,0297	69,5	4,009	40	2,308	14,75	0,851	54,75	3,159	0,719	33,7	0,269
	214	0,4238	13,5	0,0267	68,5	3,952	44	2,538	12,25	0,707	56,25	3,245	0,764	37,4	0,218
	227,5	0,4505	13,5	0,0267	68	3,923	47	2,711	10,50	0,606	56,50	3,259	0,805	37,4	0,186
	241	0,4772	14	0,0277	68	3,923	49	2,827	9,50	0,548	58,50	3,375	0,847	36,1	0,162
	255	0,5050	12,5	0,0248	68	3,923	52	3,000	8,00	0,462	60,00	3,461	0,890	40,4	0,133
	267,5	0,5297	12,5	0,0248	68	3,923	54	3,115	7,00	0,404	61,00	3,519	0,930	40,4	0,115
	280	0,5545	13	0,0257	67	3,865	56	3,231	5,50	0,317	61,50	3,548	0,970	38,8	0,089
	293	0,5802	12	0,0238	66,5	3,836	58	3,346	4,25	0,245	62,25	3,591	1,012	42,1	0,068
	305	0,6040	12	0,0238	66,5	3,836	59,5	3,433	3,50	0,202	63,00	3,634	1,051	42,1	0,056
	317	0,6277	11	0,0218	66	3,808	60,5	3,490	2,75	0,159	63,25	3,649	1,090	45,9	0,043
	328	0,6495	12	0,0238	67	3,865	62	3,577	2,50	0,144	64,50	3,721	1,126	42,1	0,039
	340	0,6733	12	0,0238	67	3,865	64	3,692	1,50	0,087	65,50	3,779	1,165	42,1	0,023
	352	0,6970	11	0,0218	66,5	3,836	64,5	3,721	1,00	0,058	65,50	3,779	1,205	45,9	0,015
	363	0,7188			66,5	3,836	65,5	3,779	0,50	0,029	66,00	3,808	1,242		0,008

(1) The estimated L^* at t = 0,0135 is lower than L_i^* (L_i^* = 0,307). This is due to rounding-off errors, inaccuracies in the measurement, and the fact that the instantaneous L^* is determined by means of a standard burning rate law that does not account for dynamic effects. Moreover, 1 mm difference in the distance from the propellant surface to the nozzle end plate gives a difference in L^* of 0,213 m. The results in column "Estimated L^*" are considered reasonable.

Table 10. Results of L* burner tests nos. 952 and 953 (D = 10 cm; propellant: ARP)

Test no.	Time		Period		Peak Pressure		Minimum Pressure		Pressure Amplitude		Mean Pressure		Estimated L^*	F	$\Delta p/\bar{p}$
	(mm)	(s)	(mm)	(s)	(mm)	(MPa)	(mm)	(MPa)	(mm)	(MPa)	(mm)	(MPa)	(m)	(s^{-1})	
952	5,7	0,011	16,8	0,033	54,8	3,161	42	2,423	6,4	0,369	48,4	2,792	1,484	30,36	0,132
	22,5	0,044	14,5	0,028	53,7	3,098	48,5	2,798	2,6	0,150	51,1	2,948	1,529	35,17	0,051
	37	0,073	16	0,031	54,2	3,127	49,2	2,838	2,5	0,144	51,7	2,982	1,568	31,88	0,048
	53	0,104	16,9	0,033	52,5	3,029	50	2,884	1,25	0,072	51,25	2,956	1,611	30,18	0,024
	69,9	0,137			51,5	2,971							1,657		
953	65,5	0,128	15,7	0,031	61	3,519	25,5	1,471	17,75	1,024	43,25	2,495	0,249	32,66	0,410
	81,2	0,158	25	0,049	63,5	3,663	23	1,327	20,25	1,168	43,25	2,495	0,314	20,51	0,468
	106,2	0,207	20	0,039	66,5	3,836	25	1,442	20,75	1,197	45,75	2,639	0,368	25,64	0,454
	126,2	0,246	18	0,035	69	3,980	28	1,515	20,50	1,183	48,50	2,798	0,418	28,49	0,423
	144,2	0,281	16,8	0,033	69,5	4,009	32,5	1,875	18,50	1,067	51,00	2,942	0,466	30,52	0,363
	161	0,314	15	0,029	70	4,038	36,5	2,106	16,75	0,966	53,25	3,072	0,515	34,19	0,315
	176	0,343	14	0,027	69,5	4,009	41	2,365	14,25	0,822	55,25	3,187	0,558	36,63	0,258
	190	0,371	13	0,025	69,5	4,009	46,5	2,682	11,50	0,663	58,00	3,346	0,599	39,45	0,198
	203	0,396	13	0,025	69,5	4,009	50	2,884	9,75	0,562	59,75	3,447	0,639	39,45	0,169
	216	0,421	11	0,021	69	3,980	53,5	3,086	7,75	0,447	61,25	3,533	0,678	46,62	0,127
	227	0,443	12,8	0,025	69	3,980	56	3,230	6,50	0,375	62,50	3,505	0,712	40,07	0,104
	239,8	0,468	12	0,023	67,5	3,894	58,5	3,375	4,50	0,260	63,00	3,634	0,753	42,73	0,071
	251,8	0,491	11,2	0,022	67,5	3,894	61	3,519	3,25	0,187	64,25	3,706	0,790	45,79	0,051
	263	0,513	11,5	0,022	68	3,923	63	3,634	2,50	0,144	65,50	3,778	0,827	44,59	0,038
	274,5	0,535	11,5	0,022	68	3,923	64,5	3,721	1,75	0,101	66,25	3,822	0,864	44,59	0,027
	286	0,558	11,3	0,022	68	3,923	65,2	3,761	1,40	0,081	66,60	3,842	0,901	45,38	0,021
	297,3	0,580	10,5	0,020	67,5	3,894	66,5	3,836	0,50	0,029	67,00	3,865	0,938	48,84	0,007
	307,8	0,600	10	0,020	67,5	3,894	66	3,807	0,75	0,043	66,75	3,851	0,972	51,28	0,011
	317,8	0,620	11,7	0,023	68	3,923	67,5	3,894	0,25	0,014	67,75	3,908	1,006	43,83	0,004
	329,5	0,643	10,5	0,020	68,5	3,952	68	3,923	0,25	0,014	68,25	3,937	1,045	48,84	0,004
	340	0,663			69	3,980							1,080		

Table 11. Results of L^* burner tests nos. 955 and 956 (D = 5 cm; propellant: ARP)

Test no.	Time		Period		Peak Pressure		Minimum Pressure		Pressure Amplitude		Mean Pressure		Estimated $L^{*(1)}$	F	$\Delta p/\bar{p}$
	(mm)	(s)	(mm)	(s)	(mm)	(MPa)	(mm)	(MPa)	(mm)	(MPa)	(mm)	(MPa)	(m)	(s^{-1})	
955	7,2	0,014	4,3	0,008	10	0,5769	8,5	0,4903	0,75	0,0433	9,25	0,5336	0,193	119,26	0,0811
	11,5	0,022	8,3	0,016	9,5	0,5480	8,5	0,4903	0,5	0,0288	9	0,5192	0,198	61,78	0,0556
	19,8	0,039	7,4	0,014	9	0,5192	7,5	0,4326	0,75	0,0433	8,25	0,4759	0,208	69,30	0,0909
	27,2	0,053	7,6	0,015	9,5	0,5480	8	0,4615	0,75	0,0433	8,75	0,5048	0,217	67,47	0,0857
	34,8	0,068	7,4	0,014	10	0,5769	9	0,5192	0,5	0,0288	9,5	0,5480	0,227	69,30	0,0526
	42,2	0,082	6,8	0,013	10	0,5769	9,2	0,5307	0,4	0,0231	9,6	0,5538	0,236	75,41	0,0417
	49	0,096			11,5	0,6634	9,5	0,5480	1	0,0577	10,5	0,6057	0,245		0,0952
	110	0,215	56,5	0,110	29	1,6729	19	1,0960	5	0,2884	24	1,3845	0,330	9,08	0,2038
	165,5	0,323	52,5	0,102	32	1,8460	15	0,8653	8,5	0,4903	23,5	1,3556	0,453	9,77	0,3617
	218	0,425	48,2	0,094	44,5	2,5670	12	0,6922	16,25	0,9374	28,25	1,6296	0,566	10,64	0,5752
	266,2	0,513	32,8	0,064	48,5	2,7978	18,5	1,0672	15	0,8653	33,5	1,9325	0,681	15,63	0,4478
	299	0,583	24	0,047	54	3,1151	25	1,4422	14,5	0,8364	39,5	2,2786	0,767	21,73	0,3671
	323	0,630	17,5	0,034	58	3,3458	36	2,0767	11	0,6345	47	2,7113	0,836	29,30	0,2340
	340,5	0,664	14,7	0,029	60	3,4612	46,5	2,6824	6,75	0,3894	53,25	3,0718	0,891	34,88	0,1268
	355,2	0,693	12,8	0,025	61,5	3,5477	55	3,1727	3,25	0,1875	58,25	3,3602	0,941	40,06	0,0558
	368	0,718	10	0,020	63,5	3,6631	61,5	3,5477	1	0,0577	62,5	3,6054	0,986	51,28	0,0160
	378	0,737	10	0,020	65,2	3,7611	65	3,7496	0,1	0,0058	65,1	3,7554	1,024	51,28	0,0015
	388	0,757			67								1,063		
956	7	0,014	20,1	0,039	46	2,6536	37,5	2,1632	4,25	0,2452	41,75	2,4084	0,801	25,47	0,1018
	27,1	0,053	14,1	0,028	50,5	2,9132	47	2,7113	1,75	0,1010	48,75	2,8122	0,854	36,31	0,0359
	41,2	0,080	17,3	0,034	50,5	2,9132	48	2,7689	1,25	0,0721	49,25	2,8410	0,895	29,60	0,0254
	58,5	0,114			50,5	2,9132	50	2,8843	0,25	0,0144	50,25	2,8987	0,945		0,0050

1) If one ignores the propellant consumed during chuffing, and one calculates the L^* starting from L_i^*, one finds in test no. 955, at t = 0,014, L^* = 0,356 m. However, though it was not well possible to determine how much propellant was consumed during chuffing, it is certain that some propellant was consumed. The estimated L^* values are based on the L_f^*, and calculated backwards.

FIG. 11
Definitions for
Data Reduction

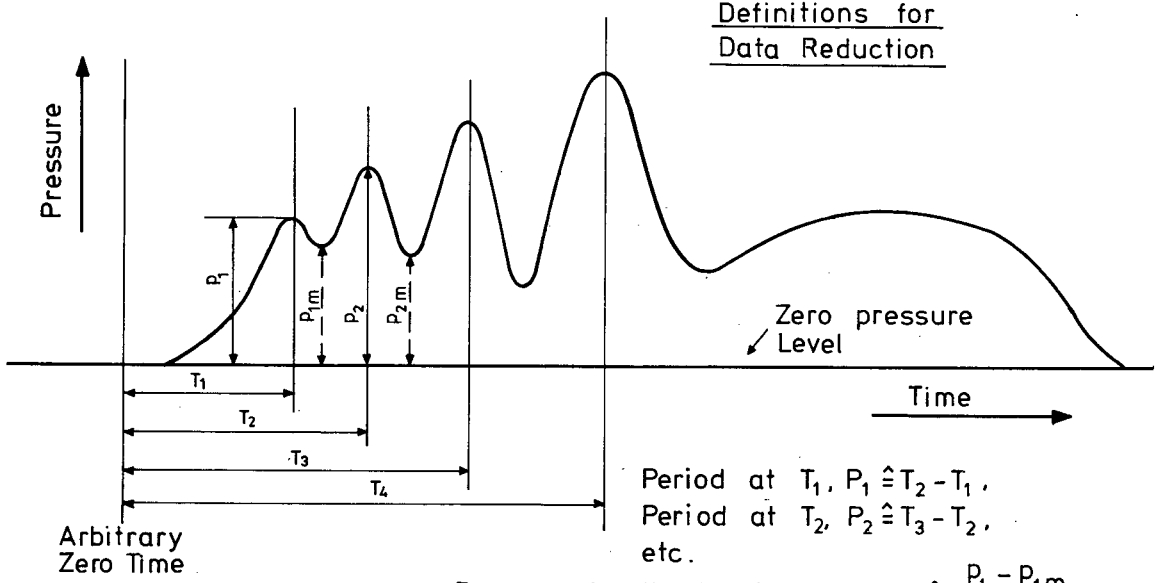

Period at T_1, $P_1 \hat{=} T_2 - T_1$,
Period at T_2, $P_2 \hat{=} T_3 - T_2$,
etc.

Pressure Amplitude at T_1, $\Delta p_{T_1} \hat{=} \frac{P_1 - P_{1m}}{2}$

Pressure Amplitude at T_2, $\Delta p_{T_2} \hat{=} \frac{P_2 - P_{2m}}{2}$

Mean Pressure at T_1, $\bar{p}_1 = \frac{P_1 + P_{1m}}{2}$

Mean Pressure at T_2, $\bar{p}_2 = \frac{P_2 + P_{2m}}{2}$

the period at the time T_i,P_i. The minimum pressure during the period P_i is p_{im} and the mean pressure $\bar{p}_i$ at T_i follows from

$$\bar{p}_i = (p_i + p_{im})/2 \tag{5-1}$$

Many other definitions for the mean pressure were possible, but none had definite advantages that made its choice preferable. The advantage of the simple definition used here, was ease of application for "manual" data reduction, which was not the case, for example, for an integral formulation.

In a similar manner the pressure amplitude Δp_i at T_i is defined as

$$\Delta p_i = (p_i - p_{im})/2 \tag{5-2}$$

Here again, other definitions were conceivable. However, regardless of the definition used, it is important to reduce all data in a consistent manner.

The Estimated L^* value

Tables 7 through 11 present estimated values of L^* obtained by use of the burning rate equation for ARP propellant [1]:

$$r = 6{,}61\ p_c^{0{,}5472} \tag{5-3}$$

where r is the burning rate in $mm.s^{-1}$ and p_c is the pressure in MPa. This standard exponential relationship is valid only for steady pressures and in cases concerned with rapid pressure transients, it is known to be inaccurate. In fact, one of the goals of this investigation was to obtain a better understanding of the dynamic combustion of solid propellants.

Since better relationships are lacking, Eq. (5-3) was used to determine the mean burning rate*).

For p_c the mean value during the particular interval was taken and used to calculate incremental changes in L^* for that particular time interval. In many cases, where instantaneous L^*-values were desired, the ignition was followed by one or more chuffs before continuous burning, either steady or oscillatory occurred, and it was very difficult to reliably determine the change in L^* over the period of chuffing. However, in all cases of interest continuous burning took place until all propellant was consumed; therefore, the estimate of instantaneous L^* was based on the L^* at burnout, L^*_f, and by going back in time, L^* was calculated for any desired instant.

In some cases it was possible to estimate L^* by starting from the initial L^* value, L^*_i. Usually, the corresponding L^* values found in these different ways, differed because of inaccuracies in pressure measurement, time measurement, measured propellant thickness, and distance, ℓ, to the nozzle, plus the fact that mean values were used. Moreover, an important cause for inaccuracies in estimated L^* was the use of the steady state burning rate equation.

For these reasons there are several instances in the column "Estimated L^*" of Tables 7 through 11, where L^* values exceed L^* or are smaller than L^*_i.

Observed pressure amplitudes and frequencies

Pressure oscillations were observed during seven tests, all with ARP propellant. According to the elementary theory of L^* oscillations, given in Reference 1, Section 4, the growth constant α is related to a

---

*) Some equations exist specifically for transients but they are complex and the accuracy of the results involves a number of assumptions.

dimensionless pressure amplitude, $\Delta p/\bar{p}$. In the derivation it is assumed that the mean pressure $\bar{p}$ remained constant. The data in Tables 7 through 11 showed this was not the case with many of the present tests. However, although mean pressure varied during the tests, the theory given in Reference 1, was applied because better theories are presently lacking. Tables 7 through 11 thus list both the pressure amplitude Δp and the dimensionless pressure amplitude $\Delta p/\bar{p}$.

The observed frequency F which is proportional to the imaginary part of the response function $R_b^{(i)}$ is also given in the Tables 7 through 11, and both the observed pressure amplitudes $\Delta p/\bar{p}$ and frequencies F are plotted in Figs. 12 through 23. The time coordinate in these Figures is not based on the arbitrary reference time used in the Tables 7 through 11, but on the first pressure peak. For test no. 936, with three successive groups of oscillations, different reference times were assigned to each group but for each group, the time is measured from the first pressure peak in that specific group of oscillations.

The plots of $\Delta p/\bar{p}$ versus time indicate that in nearly all cases the oscillations start at full amplitude $\Delta p/\bar{p}$. This is also seen in the Figs. 4 through 10 and only in test no. 955, Fig. 21, there is a clearly growing amplitude $\Delta p/\bar{p}$ during the first 0,4 s. Tests nos. 951 and 953, Figs. 16 and 19, gave some indication of a growing amplitude. The frequency F increases with time in most cases; however, for tests nos. 952 and 956, Figs. 18 and 23, it is not possible to draw definite conclusions about the variation of frequency with time because of the limited data points available and the large data scatter. In some tests the results suggest a linear relationship between frequency and time: tests nos. 936^{III}, 950 and 951, Figs. 13, 15, and 17. Test no. 953, Fig. 20, also suggests linear relationships; however, there are discontinuities. Test no. 955, Fig. 22, suggests linear relationships, especially for $t < 0{,}125$ s and $t > 0{,}5$ s, but for $0{,}125\ s < t < 0{,}5$ s the frequency increases only very slowly.

According to the mathematical description of L^* oscillations (Reference 1, Section 4), the angular frequency,

$$\omega = 2\pi F \tag{5-4}$$

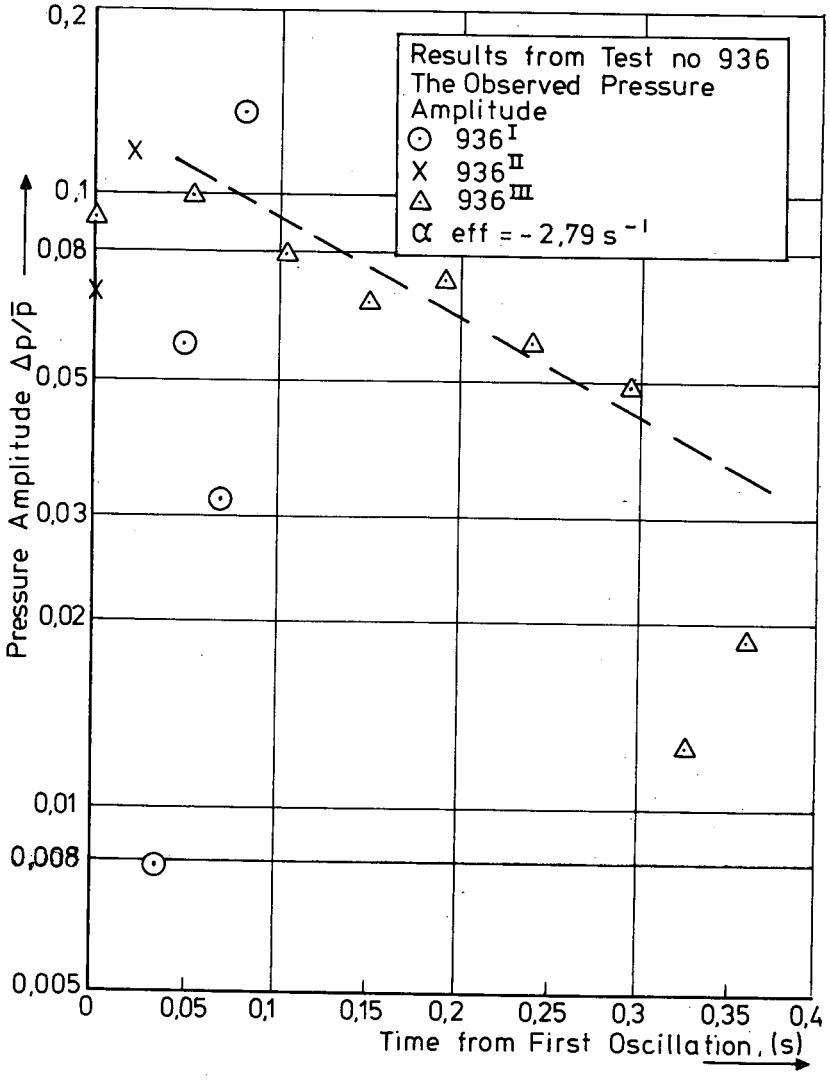

Figure 12. Variation of normalized oscillation pressure amplitude with oscillation time. Test no. 936.

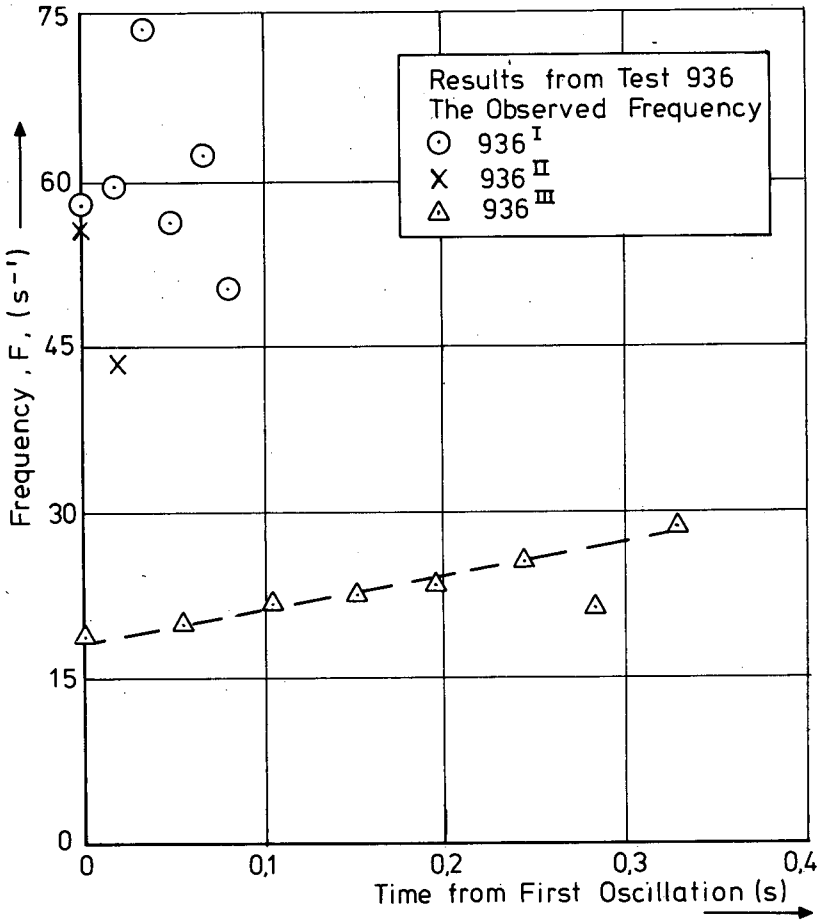

Figure 13. Variation of oscillation frequency with oscillation time. Test no. 936.

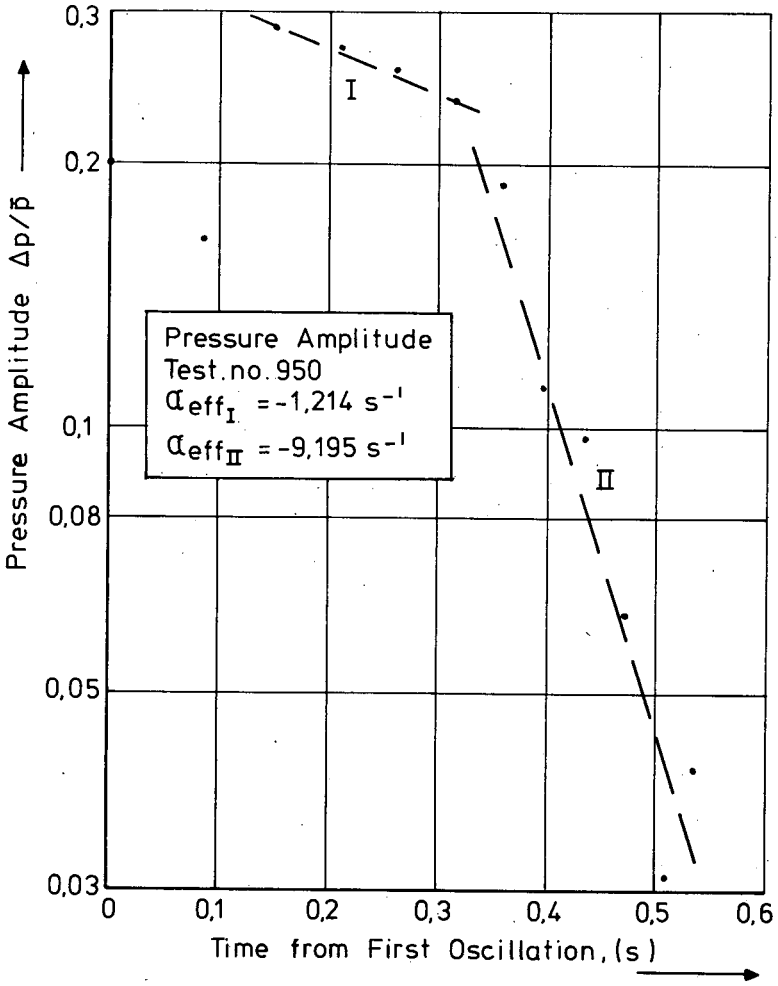

Figure 14. Variation of normalized oscillation pressure amplitude with oscillation time. Test no. 950.

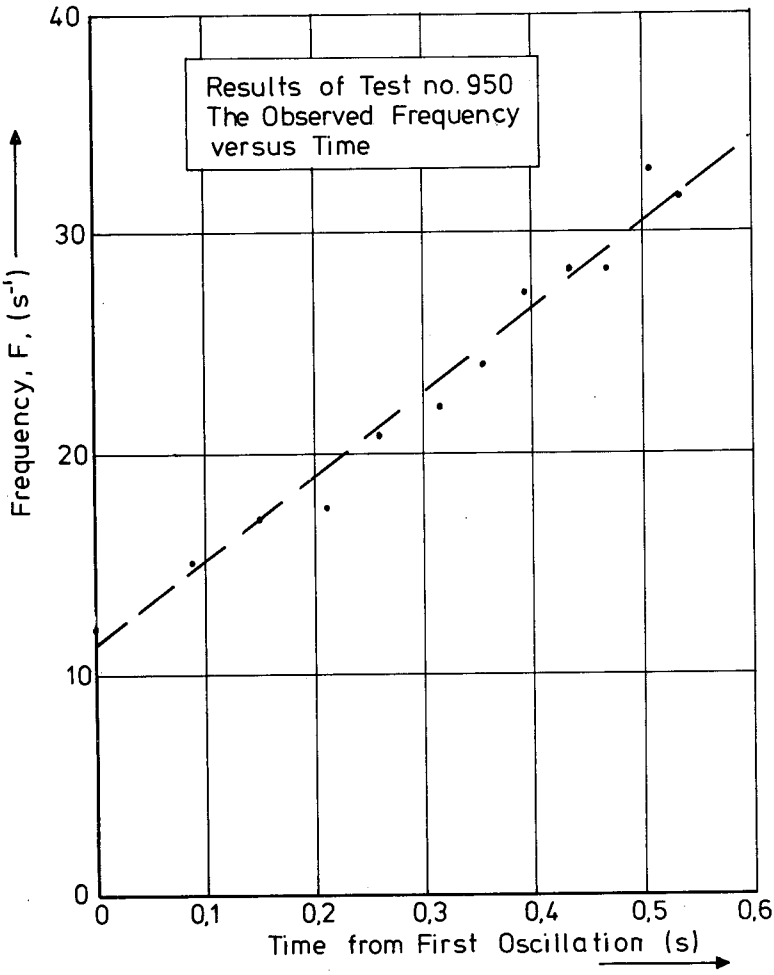

Figure 15. Variation of oscillation frequency with oscillation time. Test no. 950.

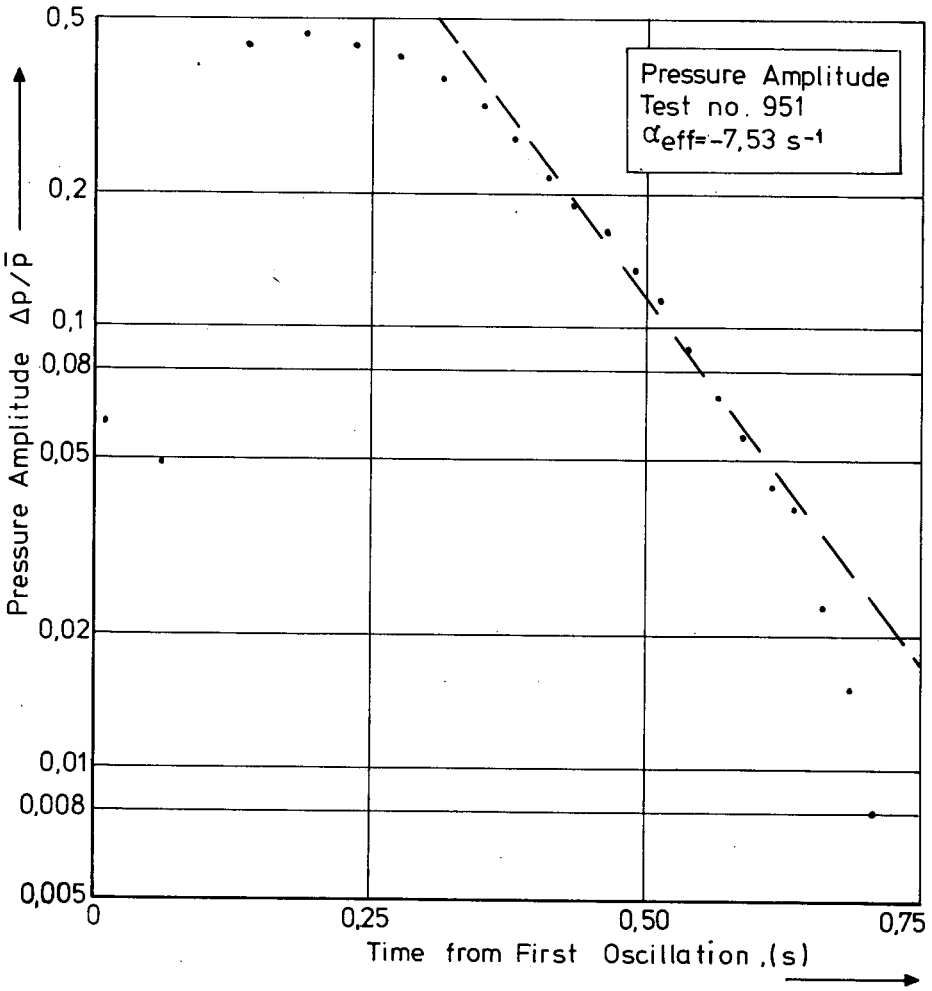

Figure 16. Variation of normalized oscillation pressure amplitude with oscillation time. Test no. 951.

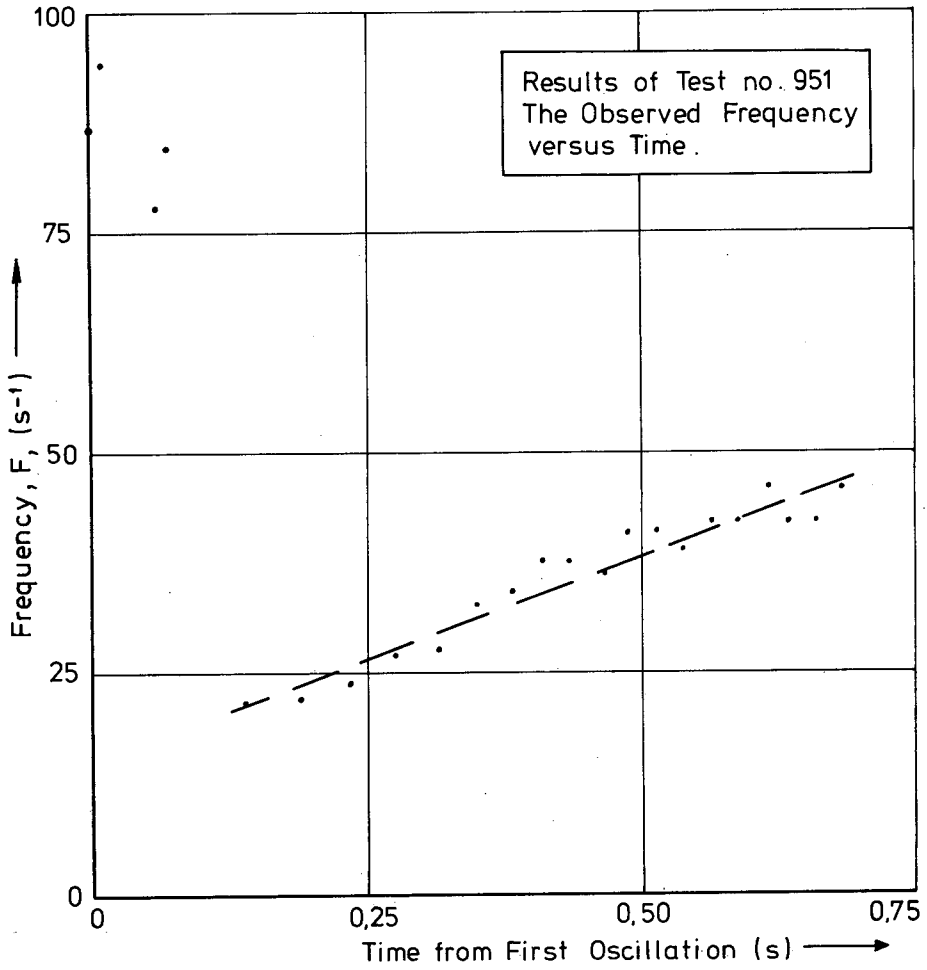

Figure 17. Variation of oscillation frequency with oscillation time. Test no. 951.

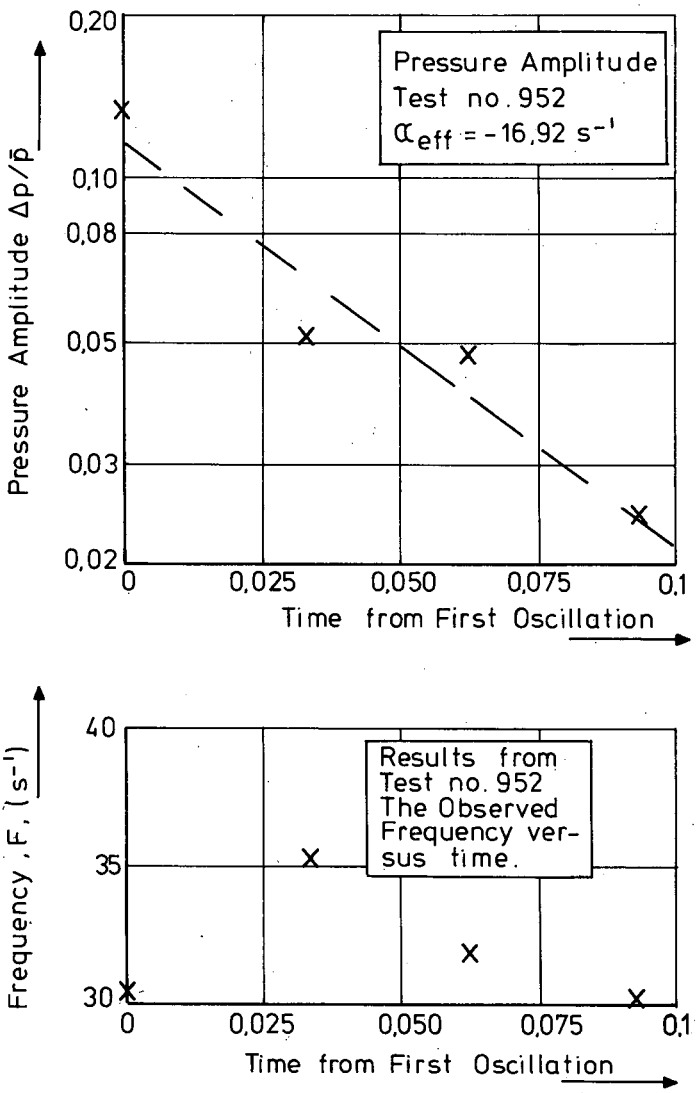

Figure 18. Variation of normalized oscillation pressure amplitude and frequency with oscillation time. Test no. 952.

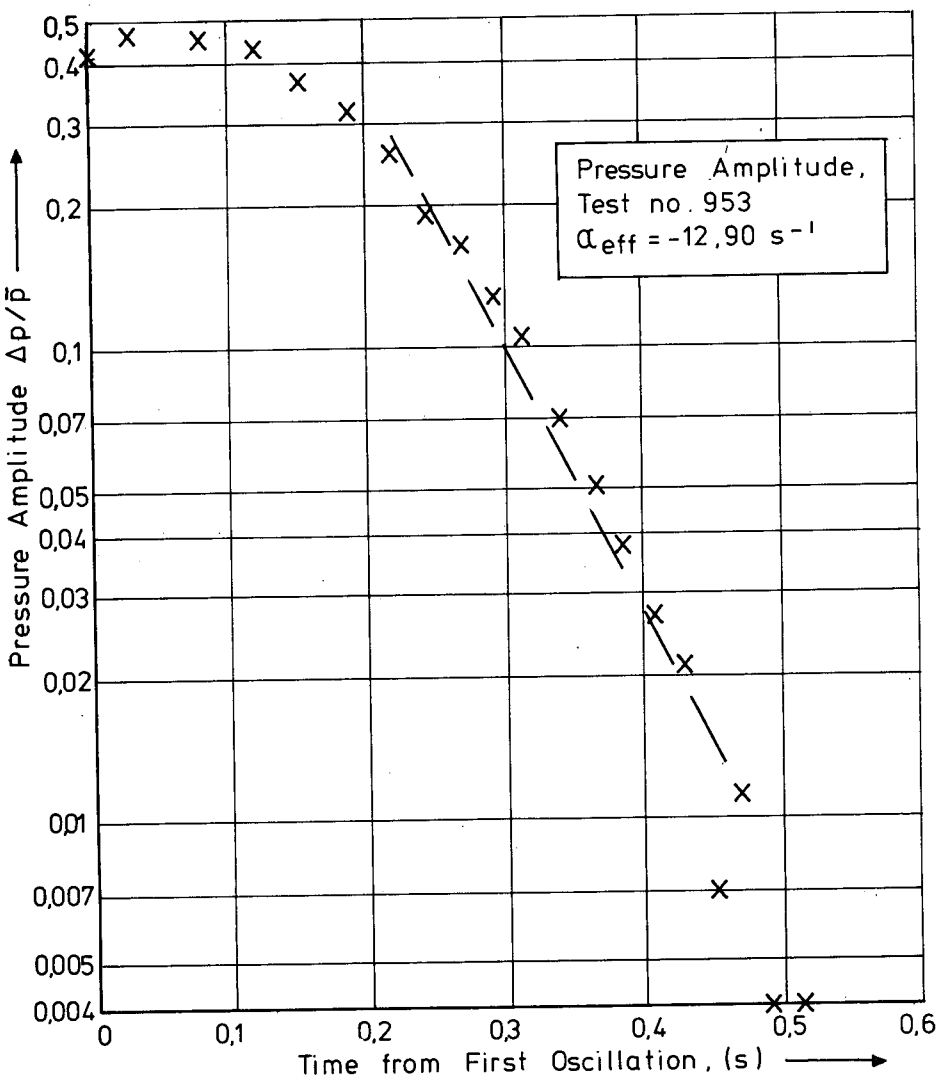

Figure 19. Variation of normalized oscillation pressure amplitude with oscillation time. Test no. 953.

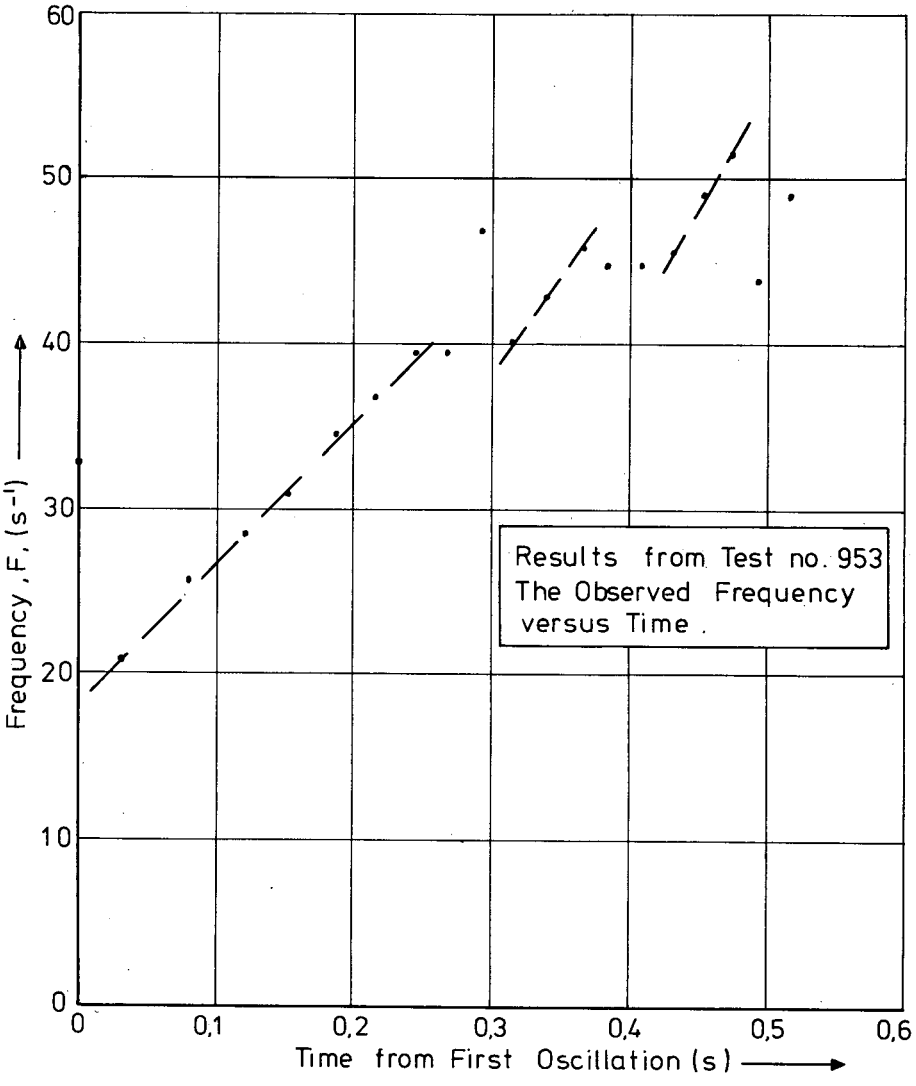

Figure 20. Variation of oscillation frequency with oscillation time. Test no. 953.

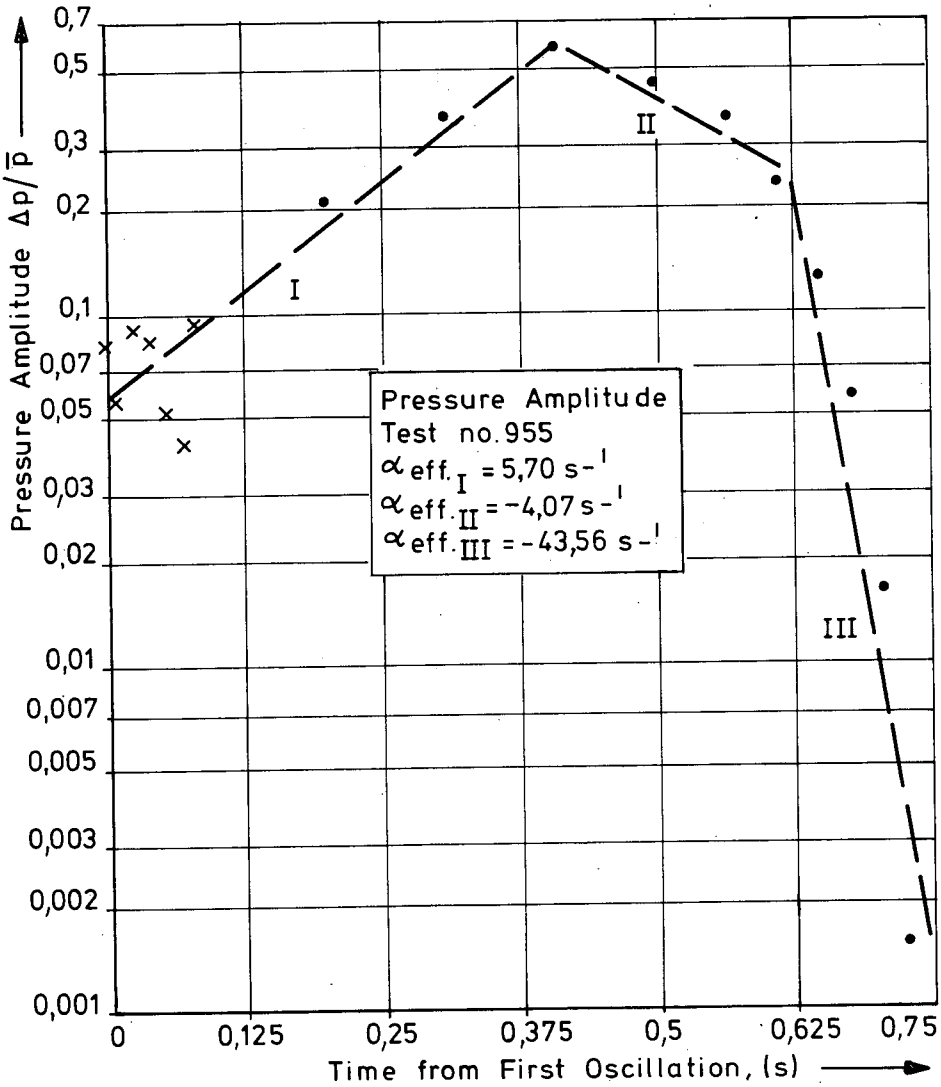

Figure 21. Variation of normalized oscillation pressure amplitude with oscillation time. Test no. 955.

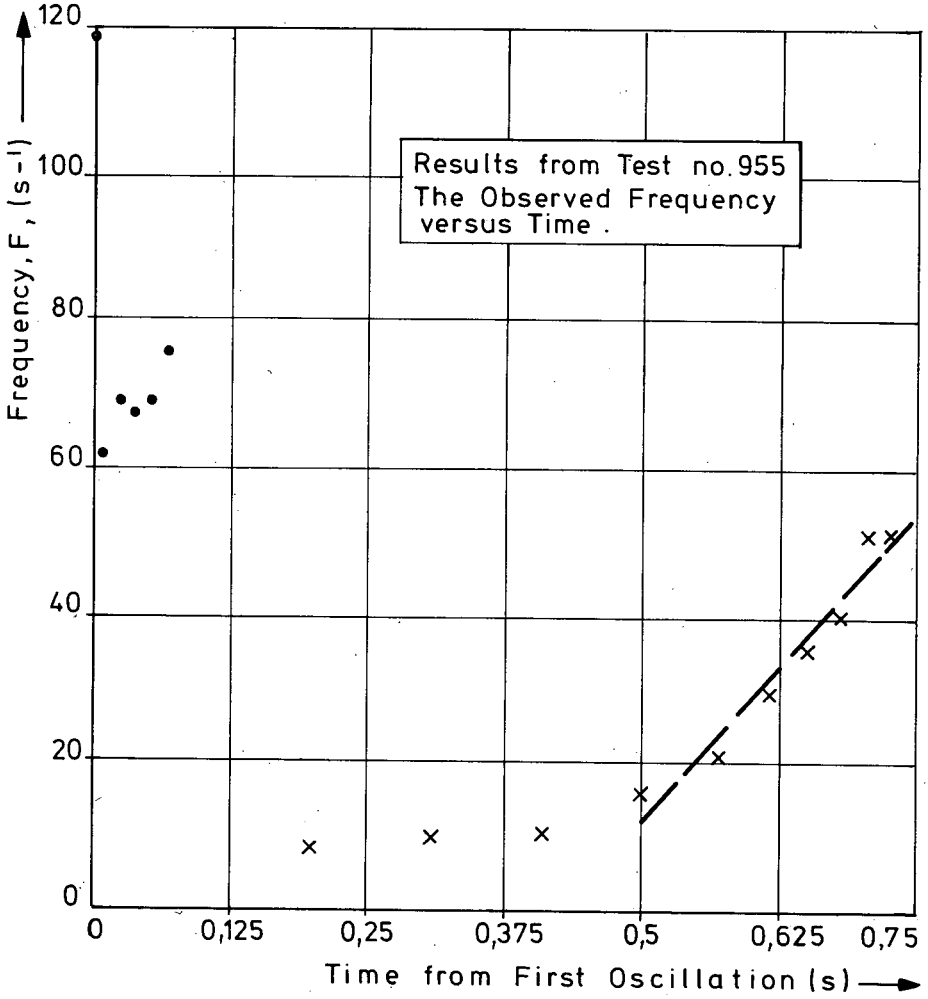

Figure 22. Variation of oscillation frequency with oscillation time. Test no. 955.

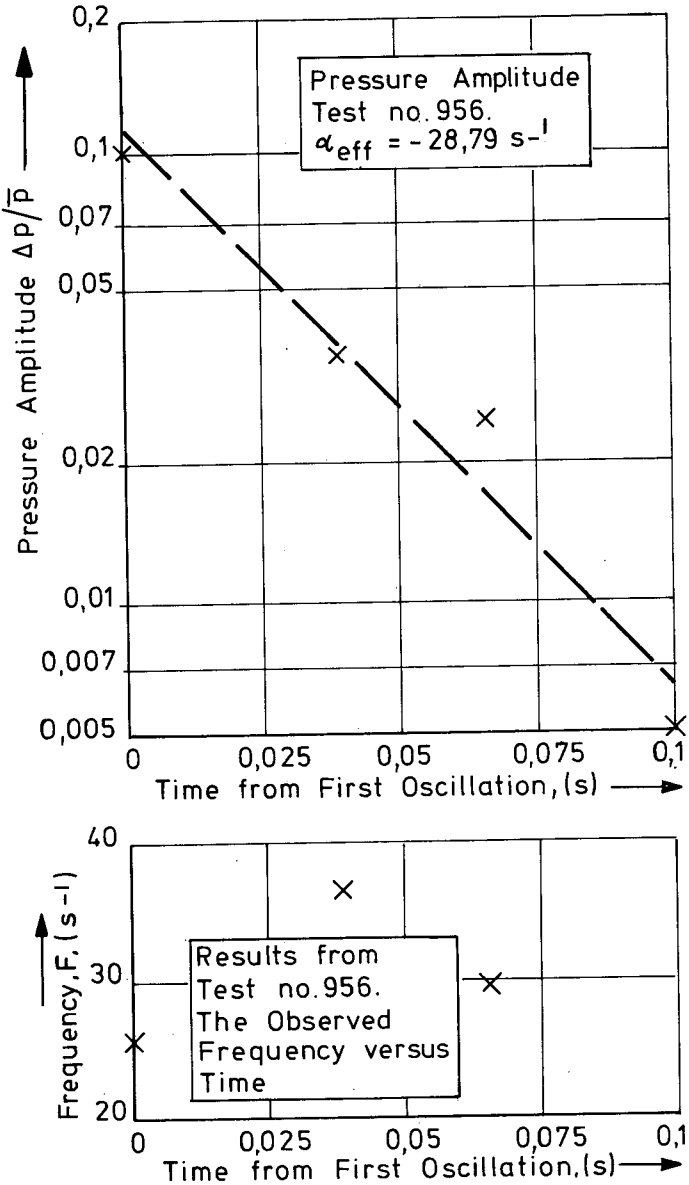

Figure 23. Variation of normalized oscillation pressure amplitude and frequency with oscillation time. Test no. 956.

determines the imaginary part of the response function $R_b^{(i)}$. Thus from these experimental data one might deduce the imaginary part of the response function. The real part of the response function $R_b^{(r)}$ is determined by the growth constant α, which follows from

$$\alpha = \mathrm{Re}\left[\left(\ln\left\{\frac{\Delta p}{\bar{p}}\right\} - \ln\left\{\frac{\Delta p}{\bar{p}}\right\}_o\right) / \left(t - t_o\right)\right] \tag{5-5}$$

where $\Delta p/\bar{p}$ is the pressure amplitude at time t and $(\Delta p/\bar{p})_o$ is the pressure amplitude at time t_o. α obtained in this manner, is the effective growth constant α_{eff}, which is the difference between the propellant growth constant α and the decay constant α_d,

$$\alpha_{eff} = \alpha - \alpha_d \tag{5-6}$$

By assuming an exponential relationship between the pressure amplitude $\Delta p/\bar{p}$ and time, α_{eff} may be estimated. The exponential relationship becomes linear if $\ln(\Delta p/\bar{p})$ is plotted versus t and α_{eff} is determined from the slope of the most probable straight line through a group of data points. In some cases two or more different values for α_{eff} were calculated during one test, i.e. Figs. 14 and 21. The groups of data points through which probable lines were drawn were chosen more or less arbitrarily. Except for test no. 955, Fig. 21, all growth constants were negative but in tests nos. 951 and 953 there was a slight indication of an $\alpha_{eff} > 0$; however, there were not enough data points to make a reliable estimate. Table 12 summarizes the results of data reduction. This table lists the independent variables $\bar{p}$ and L^*, the observed variables α_{eff} and F, and also the mean slope of the frequency dF/dt to ascertain whether there was a correlation between the frequency change and any other variable.

Table 12

The effective growth constant, frequency, and change in frequency during oscillatory combustion of ARP propellant in 5 cm and 10 cm L^* burners

Test no.	Diameter L^* burner (cm)	Effective growth constant α_{eff} (s^{-1})	Frequency range (s^{-1})	Mean frequency slope dF/dt, (s^{-2})	Mean pressure range (MPa)	L^* range (m)
936^{I}	5	-	50 - 75	-	0,31 - 0,39	0,8 - 0,84
936^{II}	5	-	45 - 55	-	0,13 - 0,23	0,85 - 0,86
936^{III}	5	- 2,79	18 - 28	22	1,95 - 2,36	1,1 - 1,5
950[1)]	10	- 1,21	12 - 33	38	1,92 - 2,36	0,43 - 0,78
950[1)]	10	- 9,20	12 - 33	38	2,36 - 2,85	0,78 - 1,13
951	10	-	87 - 93	-	0,4 - 0,49	0,29
951	10	-	77 - 84	-	0,66 - 0,72	0,32 - 0,33
951	10	- 7,53	26 - 45	49	2,18 - 3,81	0,39 - 1,24
952	10	-16,92	30 - 35	-	2,79 - 2,96	1,48 - 1,66
953	10	-12,90	20 - 40	86	2,50 - 3,35	0,31 - 0,60
953	10	-	40 - 45	119	3,53 - 3,71	0,71 - 0,79
953	10	-	45 - 51	141	3,84 - 3,85	0,90 - 0,97
955	5	5,70	60 - 75	184	0,52 - 0,55	0,36 - 0,40
955	5	- 4,07	9 - 11	7	1,38 - 1,63	0,49 - 0,73
955	5	-43,56	15 - 51	169	1,93 - 3,76	0,84 - 1,23
956	5	-28,79	25 - 36	-	2,41 - 2,90	0,80 - 0,95

1) as beased on L_i^* and calculated forward.

6. Interpretation of the results

In Section 5, Data reduction, the data are reduced to elementary quantities such as frequency F, mean pressure $\bar{p}$, amplitude Δp, and characteristic length L^*. Analysis and interpretation require a search for relations between these variables and moreover, it is desirable to obtain the response R_b of the propellant, which is determined by the circular frequency ω and the growth constant α. The measured growth constant is an effective growth constant; therefore, it is plausible to determine the propellant growth constant by comparing two similar tests. In practice the tests were not identical but some experiments were conducted at similar conditions.

Assuming that damping due to energy dissipation is mainly caused by viscosity within the gas volume, then the damping α_d is proportional to the gas volume V, i.e.

$$\alpha_d = V.C \ , \tag{6-1}$$

where C is the proportionality constant to be determined. Further, assuming that damping mainly takes place at the surface of the volume, the effect may be estimated by assuming

$$\alpha_d = C.V^{2/3}. \tag{6-2}$$

To express explicitly that damping takes place at the physical walls of the combustion volume, then the exposed surface area must be determined. The burning surface drives the oscillations and therefore, it seems reasonable to assume that damping takes place only at the cylindrical wall and at the nozzle end plate. Neglecting the nozzle surface area, the surface area exposed to combustion products is

$$S = \pi/4D^2 + \pi \ell D, \tag{6-3}$$

which equation may also be written as

$$S = \pi.(D^2/4 + L^* d_t^2/D). \tag{6-4}$$

Using this relationship the damping may be expressed as

$$\alpha_d = C\ (D^2/4 + L^*\ d_t^2/D) \tag{6-5}$$

With these assumptions the propellant growth constant may be calculated. Consider two tests yielding effective growth constants α_{eff_1} and α_{eff_2}, and assume that the propellant growth constant α is the same in both experiments, then the only difference is the damping α_d.
Comparing the results yields

$$\alpha = \alpha_{eff_1} + CT_1 \tag{6-6a}$$

$$\alpha = \alpha_{eff_2} + CT_2 \tag{6-6b}$$

Here C is the proportionality constant to be determined, while T_i is one of the terms, V_i, $V_i^{2/3}$, or $(D_i^2/4 + L_i^*\ d_{t_i}^2/D_i)$.

Taking the mean value for L^* and V, compare the results of two experiments to find a growth constant:

$$\alpha = \frac{\alpha_{eff_1} T_2 - \alpha_{eff_2} T_1}{T_2 - T_1} \qquad (6\text{-}7)$$

It should be noted that accounting only for damping, $\alpha_d > 0$ because $\alpha_d < 0$ means that the walls are driving the oscillations and this is not feasible. Another possibility is that the nozzle drives the oscillations and in that case $\alpha_d < 0$ is conceivable. If one requires $\alpha_d > 0$ then also the proportionality constant $C > 0$. Experimental results that by comparison yield $C < 0$, indicate that the nozzle is driving the oscillations, or they must be rejected for this method of estimating the propellant growth constant. Either the assumptions are not valid or the accuracy of the calculated values is not high. Equation (6-7) shows α is found from the ratio of the differences of numbers and it is accepted that this may lead to large uncertainties in the value for α.

Determination of the growth constant

The propellant growth constant may be determined from acquired data by the following procedure.
The damping depends either on the chamber volume V or on the diameter of the L^* burner, and the distance of the propellant surface to the nozzle end plate, which may be expressed as being dependent on D, L^*, and d_t, as shown in Eq. (6-5).

First, the oscillations are grouped according to their frequency range as presented in Table 13 and in Fig. 24[(a)]. Table 13 also lists other important information such as the L^* range which corresponds to the frequency range and the observed effective growth constant corresponding to that frequency and L^* range. Moreover, D and d_t are listed, while V, $V^{2/3}$, and $(D^2/4 + L^* d_t^2/D)$ are tabulated, based on the mean L^* value. From Table 13 and Fig. 24[(a)] it may be concluded that the following

Table 15

Mean Pressure Correlation

Test no.	Diameter L^* burner, D, (mm)	Throat diameter, d_t, (mm)	L^* range (m)	Mean pressure range, $\bar{p}$, (MPa)	Observed effective growth constant, α_{eff}, (s^{-1})	Mean chamber-volume, V, (mm^3)	$V^{2/3}$ (mm^2)	$D^2/4+L^*d_t^2/D$ (mm^2)
936^{III}	50	4,7	1,12 - 1,38	2,03 - 2,28	- 2,79	21687	778	1177
950^{I}	100	9,03	0,58 - 0,77	1,92 - 2,36	- 1,214	43228	1232	3050
950^{II}	100	9,03	0,77 - 1,08	2,36 - 2,85	- 9,195	59238	1520	3254
951	100	9,03	0,57 - 1,17	2,74 - 3,78	- 7,53	55717	1459	3209
952	100	9,26	1,48 - 1,61	2,79 - 2,96	-16,92	104050	2212	3825
953	100	9,03	0,56 - 0,94	3,19 - 3,67	-12,90	48032	1321	3112
955^{I}	50	4,20	0,37 - 0,73	0,53 - 1,63	5,70	7620	387	819
955^{II}	50	4,20	0,73 - 1,00	1,63 - 2,71	- 4,70	11984	524	930
955^{III}	50	4,20	1,00 - 1,19	2,71 - 3,76	-43,56	15171	613	1011
956	50	4,45	0,80 - 0,95	2,41 - 2,90	-28,79	13609	570	972

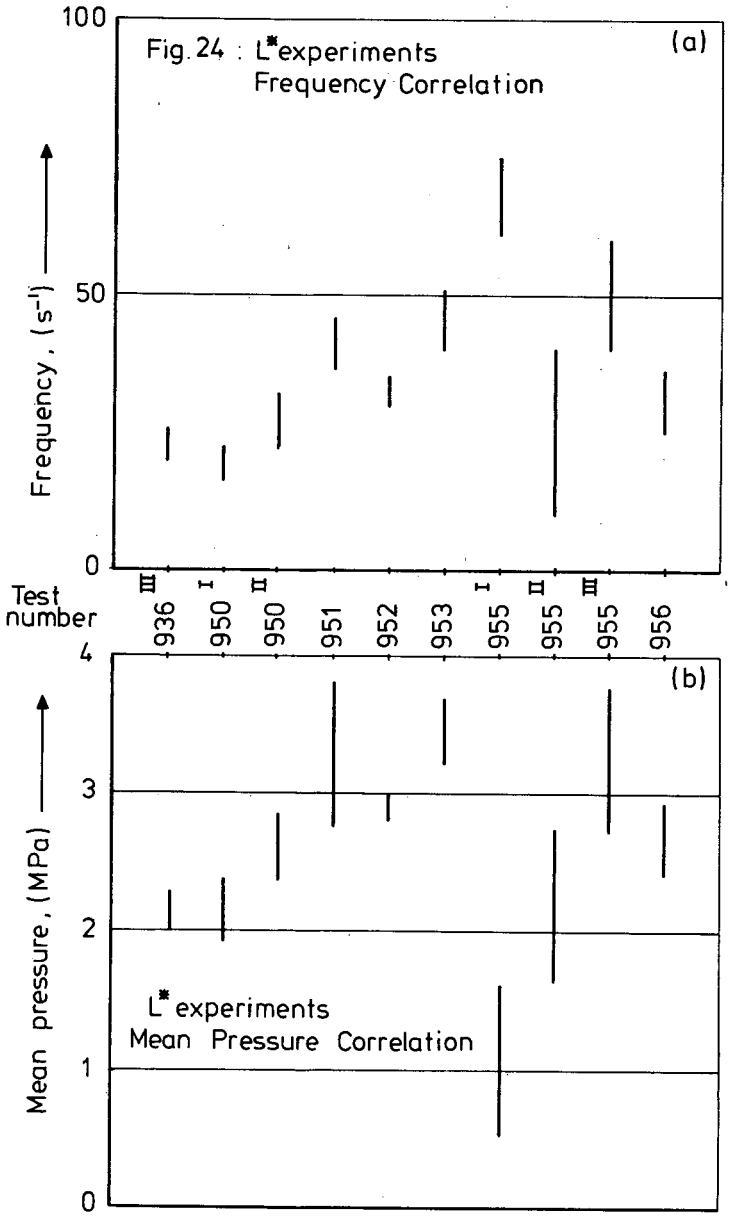

Fig. 24: Selected correlation of frequency and mean pressure by test number.

experiments have overlapping frequency ranges, so that α_d, and hence α, may be obtained from conbinations:

$936^{III}/950^{I}$; $936^{III}/950^{II}$; $936^{III}/955^{II}$;
950^{I} $/955^{II}$; 950^{II} /952 ; 950^{II} $/955^{II}$;
950^{II} /956 ; 951 /953 ; 951 $/955^{III}$;
952 $/955^{II}$; 952 /956 ; 953 $/955^{III}$;
955^{II} /956.

Only four of the combinations yield $\alpha_d > 0$ and, as $\alpha_{eff} < 0$, driving by the nozzle seems highly unlikely. Except for these four combinations the data are rejected as unsuited for this simple analysis. The four combinations that yield $\alpha_d > 0$, and the results of the calculations according to the various assumptions (damping proportional to V, $V^{2/3}$, or $(D^2/4 + L^* d_t^2/D)$ are listed in Table 14.

Table 14
Calculated propellant growth constants (frequency correlation)

Tests no.	Damping proportional to		
	V	$V^{2/3}$	$D^2/4+L^*d_t^2/D$
936^{III}/ 950^{II}	α = 0,52 s^{-1}	3,31 s^{-1}	0,70 s^{-1}
950^{II}/ 952	α = 1,38 s^{-1}	8,34 s^{-1}	35,39 s^{-1}
950^{II}/ 955^{II}	α = -2,84 s^{-1}	-1,46 s^{-1}	-2,05 s^{-1}
955^{II}/ 956	α =177,89 s^{-1}	277,32 s^{-1}	543,7 s^{-1}

Table 13

Frequency correlation

Test no.	Diameter L^* burner, D, (mm)	Throat diameter, d_t, (mm)	L^* range (m)	Observed frequency, F, (s^{-1})	Observed effective growth constant, α_{eff}, (s^{-1})	Mean chamber volume ,V, (mm^3)	$V^{2/3}$ (mm^2)	$D^2/4+L^*d_t^2/D$ (mm^2)
936^{III}	50	4,7	1,1 - 1,3	20 - 25	- 2,79	20819	757	1155
950^{I}	100	9,03	0,58 - 0,78	17 - 22	- 1,214	43549	1238	3054
950^{II}	100	9,03	0,78 - 1,13	22 - 32	- 9,20	61160	1552	3279
951	100	9,03	0,75 - 1,13	37 - 46	- 7,53	60200	1536	3266
952	100	9,26	1,48 - 1,66	30 - 35	-16,92	105733	2236	3846
953	100	9,03	0,71 - 0,97	40 - 51	-12,90	53795	1425	3185
955^{I}	50	4,20	0,36 - 0,40	61 - 75	5,70	5265	303	759
955^{I}	50	4,20	0,49 - 0,73	9 - 10	5,70	8451	415	840
955^{II}	50	4,20	0,73 - 1,0	10 - 30	- 4,07	11984	524	930
955^{III}	50	4,20	1,0 - 1,23	30 - 50	-43,56	15448	620	1018
956	50	4,45	0,80 - 0,95	25 - 36	-28,79	13609	570	972

The combination $955^{II}/956$ yields very high values for α. These experiments had already extreme values for α_{eff}, while also the numerical error may be high here as Table 13 shows: the difference of numbers of about the same value.

Though not very likely, the negative value of α, as found with the combination $950^{II}/955^{II}$ may be real, but it may also be caused by (numerical) inaccuracies.

Second, the oscillations are grouped according to their mean pressure range as presented in Table 15 and in Fig. $24^{(b)}$. The values for the L^* range in the Tables 13 and 15 differ slightly because the frequency and pressure ranges are not identical. From Fig. $24^{(b)}$ and Table 15 it may be concluded that the following experiments were conducted at approximately the same pressure ranges:

$936^{III}/950^{I}$; $936^{III}/955^{II}$; $950^{I}/955^{II}$;
$950^{II}/955^{II}$; $950^{II}/956$; $951/952$;
$951/953$; $951/955^{II}$; $951/956$;
$952/955^{III}$; $952/956$; $953/955^{III}$.

Only two of these combinations yield $\alpha_d \geq 0$ and the results of the calculations according to the various damping assumptions are listed in Table 16.

Table 16

Calculated propellant growth constants (mean pressure correlation)

Tests no.	Damping proportional to		
	V	$V^{2/3}$	$D^2/4 + L^* d_t^2/D$
$950^{II}/955^{II}$	$\alpha = -2{,}77\ s^{-1}$	$-1{,}38\ s^{-1}$	$-2{,}02\ s^{-1}$
955/952	$\alpha = -3{,}30\ s^{-1}$	$10{,}67\ s^{-1}$	$41{,}38\ s^{-1}$

The only combination that appears in both Tables 14 and 16 is the combination of the tests nos. 950^{II} and 955^{II}, and the growth constant α is negative. Whether this is due to inaccuracies, or whether the propellant growth constant for this mean pressure and frequency really is negative cannot be determined.

Assuming the damping was only marginal at the beginning of the oscillations of test no. 955^{I}, then the observed growth constant α_{eff} may equal α. Except for the tests nos. $955^{II}/956$, where extremely large values for α are found, the best agreement between the various growth constants is determined if the damping is assumed proportional to the volume, i.e. the damping is caused mainly by gas-gas instead of gas-wall interactions. On the other hand, if the growth constant varies strongly, then the assumption of damping proportional to the exposed wall surface may be perfectly valid. The combination of tests nos. 951/952 fits well with the results of the tests nos. $936^{III}/950^{II}$, $950^{II}/952$, and $950^{II}/955^{II}$ insofar as the order of magnitude of α is concerned.

Tests nos. 955^{II} and 956 yield completely different values for α. However, the α_{eff} has very small values for these tests ($-46{,}56\ s^{-1}$ and $-28{,}79\ s^{-1}$), much smaller then observed with the other experiments; therefore, it is doubtful whether the simple analysis as given in this Section is applicable.

From the results obtained it is not possible to determine whether there is a correlation between α and $\bar{p}$ or between α and F. The α values may be rather inaccurate as they follow from the ratio of the differences of two large numbers (Eq. (6-7)).
It appears, however, that for the mean pressure and frequency ranges under consideration, the growth constant of ARP propellant is at maximum at the order of some tens per second.

Assuming the changes of state isentropic, the real parts of the response function are estimated for various frequencies and pressures, and the

results are shown in Table 17. The growth constants determined from tests nos. 955^{II}/956 are omitted. No clear correlation is evident with pressure or with frequency.

Table 17

Estimated real parts of the response function, $R_b^{(r)}$. Assumed values: $\gamma = 1{,}2$; $R = 400\ m^2/(s^2K)$; $T_c = 2200\ K$

$\bar{F}$ (s^{-1})	Damping proportional to		
	V	$V^{2/3}$	$D^2/4 + L^*d_t^2/D$
9,5	0,9304	0,9304	0,9304
23,5	0,9110	0,9173	0,9121
24,75	0,9175	0,9223	0,9178
29,75	0,9195	0,9340	0,9901
68	0,9328	0,9328	0,9328
$\bar{p}$ (MPa)			
1,08	0,9218	0,9218	0,9218
2,39	0,9163	0,9169	0,9164
3,07	0,9232	0,9378	0,9986

According to the theory of L^* oscillations (De Boer and Schöyer[1], Section 4), the imaginary part of the response function,

$$R_b^{(i)} = \omega\tau^*/\delta \tag{6-8}$$

or, using the definitions of ω and τ^*, and assuming an isentropic change of state during the oscillations, i.e. $\delta = \gamma$, we have

$$R_b^{(i)} = (2\pi/(\gamma\Gamma\sqrt{RT_c})).F.L^* \tag{6-9}$$

The bracketted term in Eq. (6-9) is constant, and hence

$$R_b^{(i)} \propto F.L^*$$

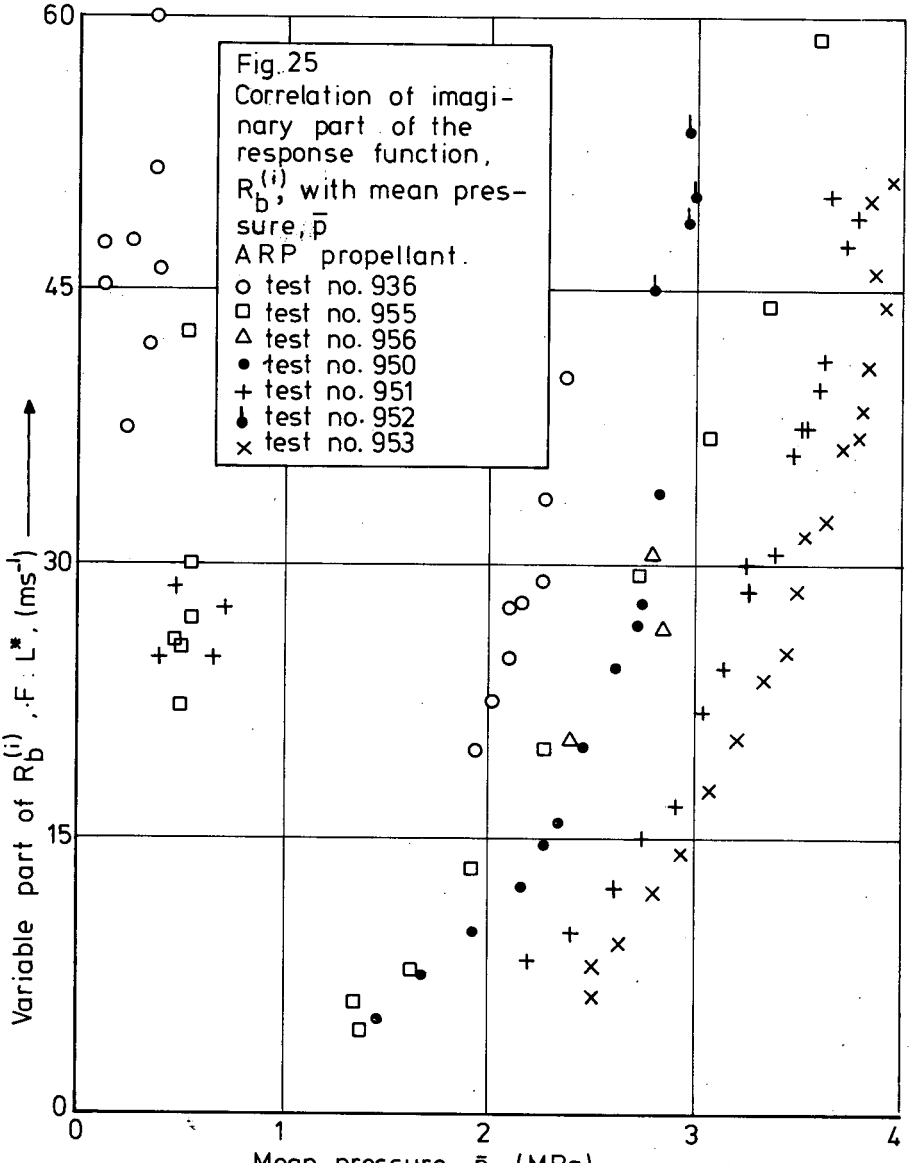
Fig. 25
Correlation of imaginary part of the response function, $R_b^{(i)}$, with mean pressure, $\bar{p}$
ARP propellant.
o test no. 936
□ test no. 955
△ test no. 956
• test no. 950
+ test no. 951
test no. 952
× test no. 953
Variable part of $R_b^{(i)}$, F. L*, (ms^{-1})
Mean pressure, $\bar{p}$, (MPa)
0
15
30
45
60
0
1
2
3
4

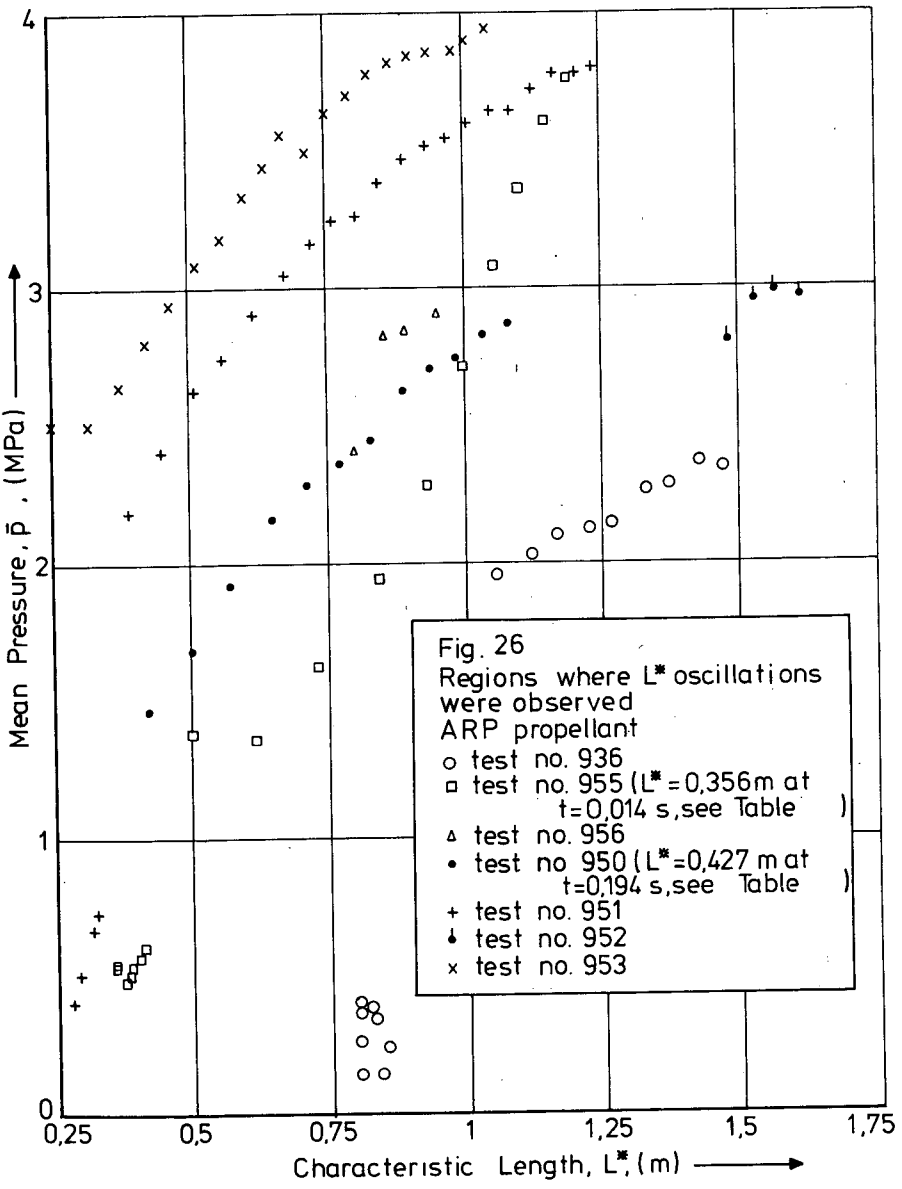
Mean Pressure, $\bar{p}$, (MPa)
Characteristic Length, L^*, (m)
0
1
2
3
4
0,25
0,5
0,75
1
1,25
1,5
1,75
Fig. 26
Regions where L^* oscillations were observed
ARP propellant
o test no. 936
□ test no. 955 (L^* = 0,356 m at t = 0,014 s, see Table)
△ test no. 956
• test no. 950 (L^* = 0,427 m at t = 0,194 s, see Table)
+ test no. 951
test no. 952
× test no. 953

This relationship is plotted in Fig. 25 versus the mean pressure. The correlation is not very good and even as the data are numerous and reasonable accurate, this may imply that the simple, one-dimensional theory does not account for enough effects and variables and does not yield an adequate description of L^* oscillations.

Acknowledging the weak correlation between $R_b^{(i)}$ and $\bar{p}$, further analysis of the experimental data was conducted to determine whether other correlations exist. It is reasonable to assume that relationships exist between the growth constant α, the mean pressure $\bar{p}$, at which oscillations occur, the frequency F, and the characteristic length L^*, of the combustion chamber. Figure 26 shows in the $L^* - \bar{p}$ plane, where oscillations were observed with experiments using ARP propellants, and the tests are identified by the plotting symbols. The Figure shows that there clearly exists a relationship between $\bar{p}$ and L^* for every experiment, but a correlation between the various experiments is not evident. The same variables, $\bar{p}$ and L^* for those regions where L^* oscillations were observed, are also plotted in Fig. 27 but on a double logarithmic scale. This Figure suggests that there are two regions where L^* oscillations may occur for ARP propellant, one region approximately: $0{,}15 \text{ MPa} < \bar{p} < 0{,}4 \text{ MPa}$ and $0{,}25 \text{ m} < L^* < 0{,}8 \text{ m}$ and the other region approximately $1{,}4 \text{ MPa} < \bar{p} < 4 \text{ MPa}$ and $0{,}25 \text{ m} < L^* < 1{,}6 \text{ m}$. The use of logarithmic scales emphasizes the division into two clearly distinghuish--able regions. Therefore, it is not clear, as yet whether L^* oscillations using ARP propellant, will not occur in the intermediate region, $0{,}4 \text{ MPa} < \bar{p} < 1{,}4 \text{ MPa}$, or whether these oscillations were not evident during the present experiments. Figure 28 shows the observed frequency F, plotted versus L^*. Again, there is a clear correlation between the data points of one experiment, but there is no clear relationship between the various experiments. Again, it appears as if the results are in two groups: a group of higher frequency oscillations, $F > 60 \text{ s}^{-1}$, $L^* < 0{,}4 \text{ m}$ and a group of lower frequency oscillations, $F < 60 \text{ s}^{-1}$. Comparing Figures 26 and 28 leads to the conclusion that at low pressure and low L^*, relatively high frequency L^* oscillations may take place, while at

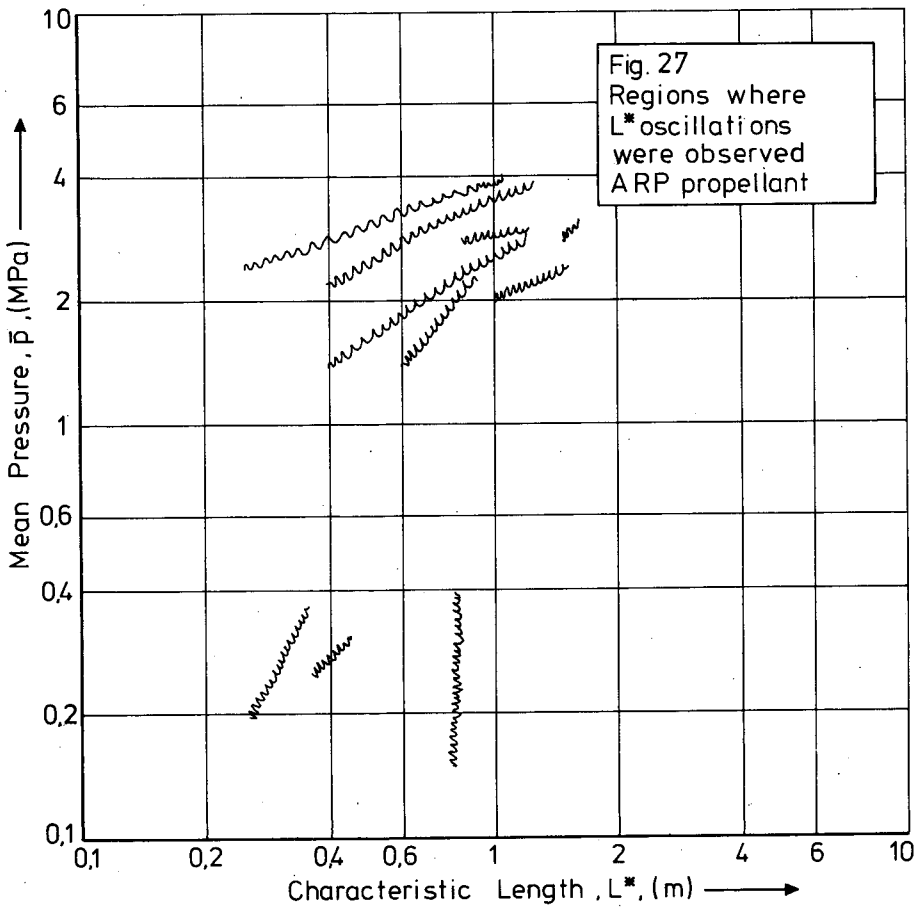
Fig. 27
Regions where
L* oscillations
were observed
ARP propellant
Mean Pressure, p̄, (MPa)
10
6
4
2
1
0,6
0,4
0,2
0,1
0,1
0,2
0,4
0,6
1
2
4
6
10
Characteristic Length, L*, (m)

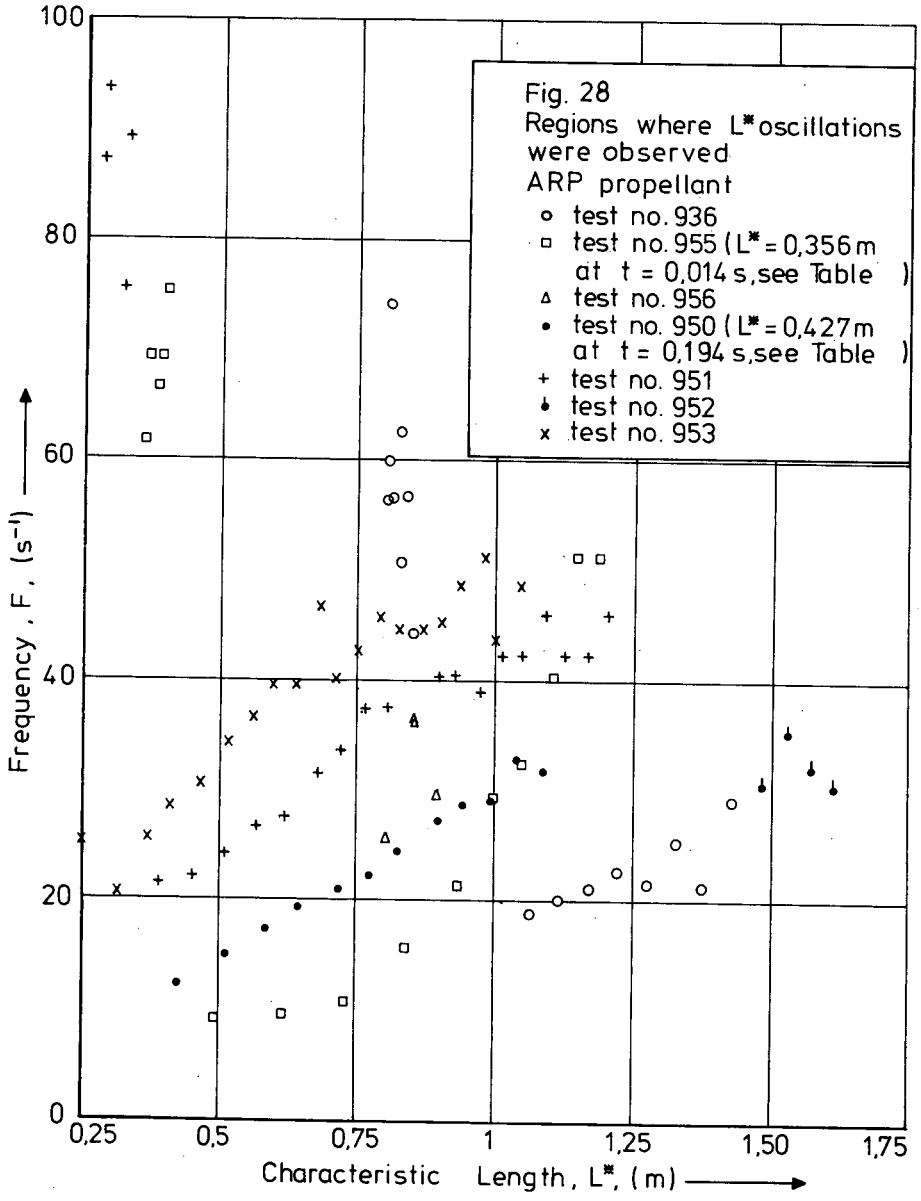
Fig. 28
Regions where L* oscillations were observed
ARP propellant
o test no. 936
□ test no. 955 (L* = 0,356 m at t = 0,014 s, see Table)
Δ test no. 956
• test no. 950 (L* = 0,427 m at t = 0,194 s, see Table)
+ test no. 951
• test no. 952
x test no. 953
Frequency, F, (s⁻¹)
100
80
60
40
20
0
0,25
0,5
0,75
1
1,25
1,50
1,75
Characteristic Length, L*, (m)

high pressure and somewhat larger L^* values, the frequency of oscillations, if oscillations occur, is somewhat lower. The data scatter, however, is large, which is not unusual for L^* experiments; Schöyer[2] and Kumar and McNamara[3], for example, show many plots in which the scatter is much larger. The data presented in this report show, however, that there is no preferred tendency either towards the 5 cm L^* burner (closed data points) or the 10 cm L^* burner (open data points). The agreement between results obtained with L^* burners of different sizes is as good as the agreement between results obtained with an L^* burner of a fixed size; hence the data are not affected by geometric scale effects.

Noting that for ARP propellant higher frequency oscillations may occur at a low mean pressure and lower frequency oscillations may occur at a somewhat higher pressure, the observed frequency versus mean pressure is plotted in Fig. 29. The "high pressure" data tend to lie on a straight line with slope of about $15{,}2 \times 10^{-6}$ m.s.kg^{-1}. The data scatter is very small compared to the results shown in Fig. 25, 26, and 28.
Figure 29 suggests that there are at least two regions in which L^* oscillations occur, although the relation between the regions is not clear. The connection between the regious was not established by the present series of experiments, nor by De Boer and Schöyer[1] with earlier experiments. A relation between mean pressure and frequency was observed by Strand[4] who presented some plots of F versus $\bar{p}$, but they lacked the strong correlation observed in Fig. 29. Moreover, Strand[4] presented his data on a double logarithmic scale. Eisel et al.[5] also published an observed pressure-frequency correlation for a metallized, cast double base propellant. Most of Eisel's data were based on work with what was called an LE-burner and which now is generally known as a T burner. Only one group of data was based on measurements with a device similar to an L^* burner. Although the T burner and L^* burner data did correlate, Eisel's data seemed to indicate that the L^* burner at the same pressure as the T burner oscillated at a somewhat lower frequency. In the pressure range up to 1,4 MPa L^* burner data indicated a slope of

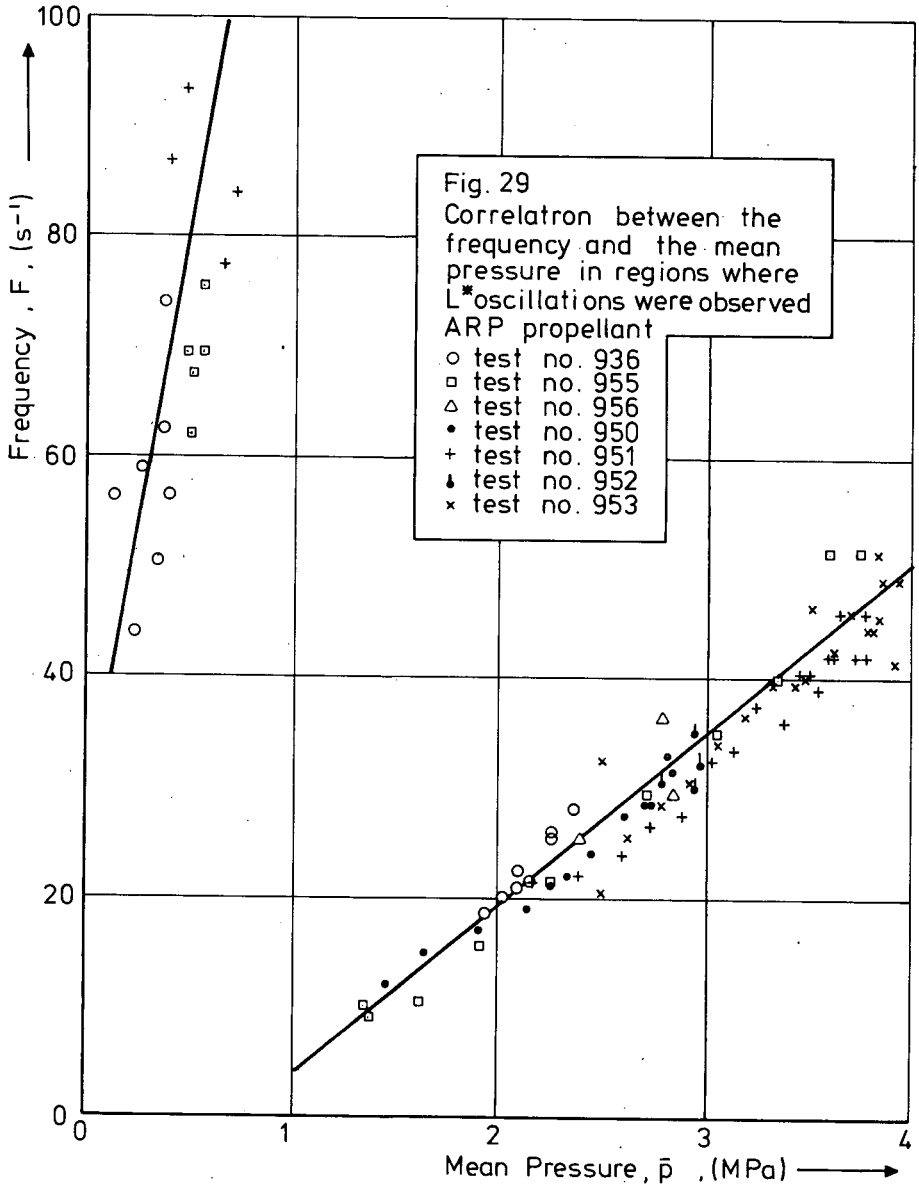
Fig. 29
Correlatron between the frequency and the mean pressure in regions where L*oscillations were observed
ARP propellant
○ test no. 936
□ test no. 955
△ test no. 956
• test no. 950
+ test no. 951
♦ test no. 952
× test no. 953
Frequency , F , (s⁻¹)
100
80
60
40
20
0
0
1
2
3
4
Mean Pressure , p̄ , (MPa)

$4{,}14 \times 10^{-6}$ m.s.kg^{-1}, which is of the same order of magnitude found here for ARP propellant. Eisel did not report a "high-frequency" - "low pressure" correlation, such as indicated in the upper left of Fig. 29. In his contribution to "Advances in Tactical Rocket Propulsion", Price[6] gave the same results and commented that the controlling mechanism for L^* burner oscillation frequency was not well understood. Moreover, he noted that L^* oscillations were usually confined to combustion pressures up to 300 to 400 psi (2,1 MPa to 2,8 MPa). In this respect it should be noted that in the present case L^* oscillations were observed in the pressure range of 1,4 MPa to 4 MPa and the frequency range of 10 s^{-1} to 50 s^{-1}. At still lower pressures up to 1 MPa, oscillations occurred at a frequency between 40 s^{-1} and 100 s^{-1}. Yount and Angelus[7] reported a pressure-frequency correlation which data covered a frequency range of 35 s^{-1} to 45 s^{-1} and a pressure range of 0,7 MPa to 1,3 MPa ($\sim$100 psi - 190 psi). More recent observations were made by Margulis et al.[8], who obtained a mean pressure-frequency correlation for internal burning cylindrical grains in rocket motors. The observed pressure range was very high for L^* oscillations: 5 MPa to 16 MPa and the frequency was 10 s^{-1} to 60 s^{-1}. It is noteworthy that the pressure-frequency correlation reported herein fits very well with the published data. Moreover, except for Margulis' data, the $\bar{p}$-F relationship was observed over a much larger pressure range than previously reported, while, to the authors' knowledge, the $\bar{p}$-F relationship at "low pressures" and "high frequencies" was not reported earlier.

7. Conclusions

- ARP propellant produced oscillatory combustion in two L^* - $\bar{p}$ regions:
  a) 0,15 MPa $< \bar{p} <$ 0,4 MPa & 0,25 m $< L^* <$ 0,8 m & 40 $s^{-1} < F <$ 100 s^{-1};
  b) 1,4 MPa $< \bar{p} <$ 4 MPa & 0,25 m $< L^* <$ 1,6 m & 10 $s^{-1} < F <$ 50 s^{-1}.

- There was a clear, linear correlation between frequency F and mean pressure $\bar{p}$, at which L^* oscillations occurred for ARP propellant; however, it was not clear whether the oscillation regions were inter-related.

- There was considerable scatter in the correlation of mean pressure $\bar{p}$, frequency F, and characteristic length L^* during the oscillations. This scatter could not be explained by the uncertainty in the L^* value.

- The propellant growth constant for ARP propellant, in the regions investigated amounted, at maximum, to a few tens per second.

- L^* oscillations for JPN were not observed for $L^* > 4{,}4$ m and $\bar{p} > 1{,}1$ MPa, nor for $L^* < 2$ m and $\bar{p} < 1$ MPa.

- Reliable, reproducible propellant ignition was achieved by use of the pyrotechnic lacquer and electrical resistance wire technique, described by De Boer and Schöyer[1].

8. List of Tables

9. List of Figures

10. References

1. R.S. de Boer and H.F.R. Schöyer, Results of L^* Instability Experiments with Double Base Rocket Propellants, Delft University of Technology, Dept. of Aerospace Engineering/Technological Laboratory TNO, Delft/Rijswijk, 1976.

2. H.F.R. Schöyer, Report on Low-Frequency Oscillatory Combustion Experiments, Daniel and Florence Guggenheim Jet Propulsion Center, California Institute of Technology, Pasadena, 1971.

3. R.N. Kumar and R.P. McNamara, Some Experiments Related to L-Star Instability in Rocket Motors, Daniel and Florence Guggenheim Jet Propulsion Center, California Institute of Technology, Pasadena, 1973.

4. L.D. Strand, Summary of a Study of the Low-Pressure Combustion of Solid Propellants, Technical Report 32-1242, Jet Propulsion Laboratory, California Institute of Technology, Pasadena, April 1968.

5. L.J. Eisel, M.D. Horton, E.W. Price and D.W. Rice, Preferred Frequency Oscillatory Combustion of Solid Propellants, AIAA-J, 7 (1964) 1319-1323.

6. E.W. Price, Review of Combustion Instability Characteristics of Solid Propellants, Chapter 5 in: Advances in Tactical Rocket Propulsion, ed. S.S. Penner, AGARD Conference Proceedings no. 1, Technivision, Maidenhead, 1968.

7. R.A. Yount and T.A. Angelus, Chuffing and Nonacoustic Instability Phenomena in Solid Propellant Rockets, AIAA-J, 7 (1964), 1307-1313.

8. V.M. Margulis, A.D. Margolin, M.E. Lévichek, P.F. Pokhil, and A.I. Larin, Self-Oscillations and Low-Frequency Instability of Solid-Propellant Combustion. Translated from a Russian Article in: Fizika Goreniya i Vzryva, 6, (1970) 162-166. Translation: Plenum Publ. Corp. New York.

Summary A series of oscillatory combustion experiments has been conducted to detect the sensitivity of double base rocket propellants for low frequency oscillations. The experiments are a continuation of earlier work by De Boer and Schöyer, and the ignition technique developed earlier, again proved to be reliable and gave reproducible results.
In the experiments reported herein two regions in the $L^* - \bar{p}$ plane were found where ARP propellant was apt to oscillate: $0,15\ MPa < \bar{p} < 0,4\ MPa$ with $0,25\ m < L^* < 0,8\ m$ and $1,4\ MPa < \bar{p} < 4\ MPa$ with $0,25\ m < L^* < 1,6\ m$ (L^* = characteristic length of the combustion chamber; $\bar{p}$ = mean pressure at oscillation). No oscillations have been observed with JPN propellant. It is conceivable that this is due to the absence of an ignition peak.
Tests that yielded oscillations are reported in detail in this report both in tabular and in graphical form.
From the data the effective growth constants have been deduced and postulating various models for damping in the combustion chamber, it has been possible to estimate the growth constant of ARP propellant. The best correlation has been obtained by assuming volumetric damping. Correlation of the response function with $\bar{p}$ has been found to be weak, like the correlations between mean pressure at oscillation and L^* and between frequency and L^*. Both 5 and 10 cm L^* burners have been used; it is of interest to note that the data scatter for the 5 cm and 10 cm burner is of the same order as the data scatter between the 5 cm and 10 cm burners. Therefore the results of the different burners agree rather well. Very good correlation has been found between frequency and mean pressure and over a much wider pressure range than previously reported. Moreover, a high frequency - low pressure correlation has been observed which, to the authors' knowlegde, has never been reported earlier.

Report LR-252; TL R 3050 II
Date: September 1977
Authors: R.S. de Boer, H.F.R. Schöyer, and H. Wolff.
Title: Results of L^*-Instability Experiments with Double Base Rocket Propellants II

Description: Combustion Stability (2102), Solid Propellant Rocket Engines (2108), Test Engines (2111), Double Base Rocket Propellants (2109), Pressure Measurements (1402).

Summary A series of oscillatory combustion experiments has been conducted to detect the sensitivity of double base rocket propellants for low frequency oscillations. The experiments are a continuation of earlier work by De Boer and Schöyer, and the ignition technique developed earlier, again proved to be reliable and gave reproducible results.
In the experiments reported herein two regions in the $L^* - \bar{p}$ plane were found where ARP propellant was apt to oscillate: $0,15\ MPa < \bar{p} < 0,4\ MPa$ with $0,25\ m < L^* < 0,8\ m$ and $1,4\ MPa < \bar{p} < 4\ MPa$ with $0,25\ m < L^* < 1,6\ m$ (L^* = characteristic length of the combustion chamber; $\bar{p}$ = mean pressure at oscillation). No oscillations have been observed with JPN propellant. It is conceivable that this is due to the absence of an ignition peak.
Tests that yielded oscillations are reported in detail in this report both in tabular and in graphical form.
From the data the effective growth constants have been deduced and postulating various models for damping in the combustion chamber, it has been possible to estimate the growth constant of ARP propellant. The best correlation has been obtained by assuming volumetric damping. Correlation of the response function with $\bar{p}$ has been found to be weak, like the correlations between mean pressure at oscillation and L^* and between frequency and L^*. Both 5 and 10 cm L^* burners have been used; it is of interest to note that the data scatter for the 5 cm and 10 cm burner is of the same order as the data scatter between the 5 cm and 10 cm burners. Therefore the results of the different burners agree rather well. Very good correlation has been found between frequency and mean pressure and over a much wider pressure range than previously reported. Moreover, a high frequency - low pressure correlation has been observed which, to the authors' knowlegde, has never been reported earlier.

Report LR-252; TL R 3050 II
Date: September 1977
Authors: R.S. de Boer, H.F.R. Schöyer, and H. Wolff.
Title: Results of L^*-Instability Experiments with Double Base Rocket Propellants II

Description: Combustion Stability (2102), Solid Propellant Rocket Engines (2108), Test Engines (2111), Double Base Rocket Propellants (2109), Pressure Measurements (1402).

Summary A series of oscillatory combustion experiments has been conducted to detect the sensitivity of double base rocket propellants for low frequency oscillations. The experiments are a continuation of earlier work by De Boer and Schöyer, and the ignition technique developed earlier, again proved to be reliable and gave reproducible results.
In the experiments reported herein two regions in the $L^* - \bar{p}$ plane were found where ARP propellant was apt to oscillate: $0,15\ MPa < \bar{p} < 0,4\ MPa$ with $0,25\ m < L^* < 0,8\ m$ and $1,4\ MPa < \bar{p} < 4\ MPa$ with $0,25\ m < L^* < 1,6\ m$ (L^* = characteristic length of the combustion chamber; $\bar{p}$ = mean pressure at oscillation). No oscillations have been observed with JPN propellant. It is conceivable that this is due to the absence of an ignition peak.
Tests that yielded oscillations are reported in detail in this report both in tabular and in graphical form.
From the data the effective growth constants have been deduced and postulating various models for damping in the combustion chamber, it has been possible to estimate the growth constant of ARP propellant. The best correlation has been obtained by assuming volumetric damping. Correlation of the response function with $\bar{p}$ has been found to be weak, like the correlations between mean pressure at oscillation and L^* and between frequency and L^*. Both 5 and 10 cm L^* burners have been used; it is of interest to note that the data scatter for the 5 cm and 10 cm burner is of the same order as the data scatter between the 5 cm and 10 cm burners. Therefore the results of the different burners agree rather well. Very good correlation has been found between frequency and mean pressure and over a much wider pressure range than previously reported. Moreover, a high frequency - low pressure correlation has been observed which, to the authors' knowledge, has never been reported earlier.

Report LR-252; TL R 3050 II
Date: September 1977
Authors: R.S. de Boer, H.F.R. Schöyer, and H. Wolff.
Title: Results of L^*-Instability Experiments with Double Base Rocket Propellants II

Description: Combustion Stability (2102), Solid Propellant Rocket Engines (2108), Test Engines (2111), Double Base Rocket Propellants (2109), Pressure Measurements (1402).

Summary A series of oscillatory combustion experiments has been conducted to detect the sensitivity of double base rocket propellants for low frequency oscillations. The experiments are a continuation of earlier work by De Boer and Schöyer, and the ignition technique developed earlier, again proved to be reliable and gave reproducible results.
In the experiments reported herein two regions in the $L^* - \bar{p}$ plane were found where ARP propellant was apt to oscillate: $0,15\ MPa < \bar{p} < 0,4\ MPa$ with $0,25\ m < L^* < 0,8\ m$ and $1,4\ MPa < \bar{p} < 4\ MPa$ with $0,25\ m < L^* < 1,6\ m$ (L^* = characteristic length of the combustion chamber; $\bar{p}$ = mean pressure at oscillation). No oscillations have been observed with JPN propellant. It is conceivable that this is due to the absence of an ignition peak.
Tests that yielded oscillations are reported in detail in this report both in tabular and in graphical form.
From the data the effective growth constants have been deduced and postulating various models for damping in the combustion chamber, it has been possible to estimate the growth constant of ARP propellant. The best correlation has been obtained by assuming volumetric damping. Correlation of the response function with $\bar{p}$ has been found to be weak, like the correlations between mean pressure at oscillation and L^* and between frequency and L^*. Both 5 and 10 cm L^* burners have been used; it is of interest to note that the data scatter for the 5 cm and 10 cm burner is of the same order as the data scatter between the 5 cm and 10 cm burners. Therefore the results of the different burners agree rather well. Very good correlation has been found between frequency and mean pressure and over a much wider pressure range than previously reported. Moreover, a high frequency - low pressure correlation has been observed which, to the authors' knowledge, has never been reported earlier.

Report LR-252; TL R 3050 II
Date: September 1977
Authors: R.S. de Boer, H.F.R. Schöyer, and H. Wolff.
Title: Results of L^*-Instability Experiments with Double Base Rocket Propellants II

Description: Combustion Stability (2102), Solid Propellant Rocket Engines (2108), Test Engines (2111), Double Base Rocket Propellants (2109), Pressure Measurements (1402).